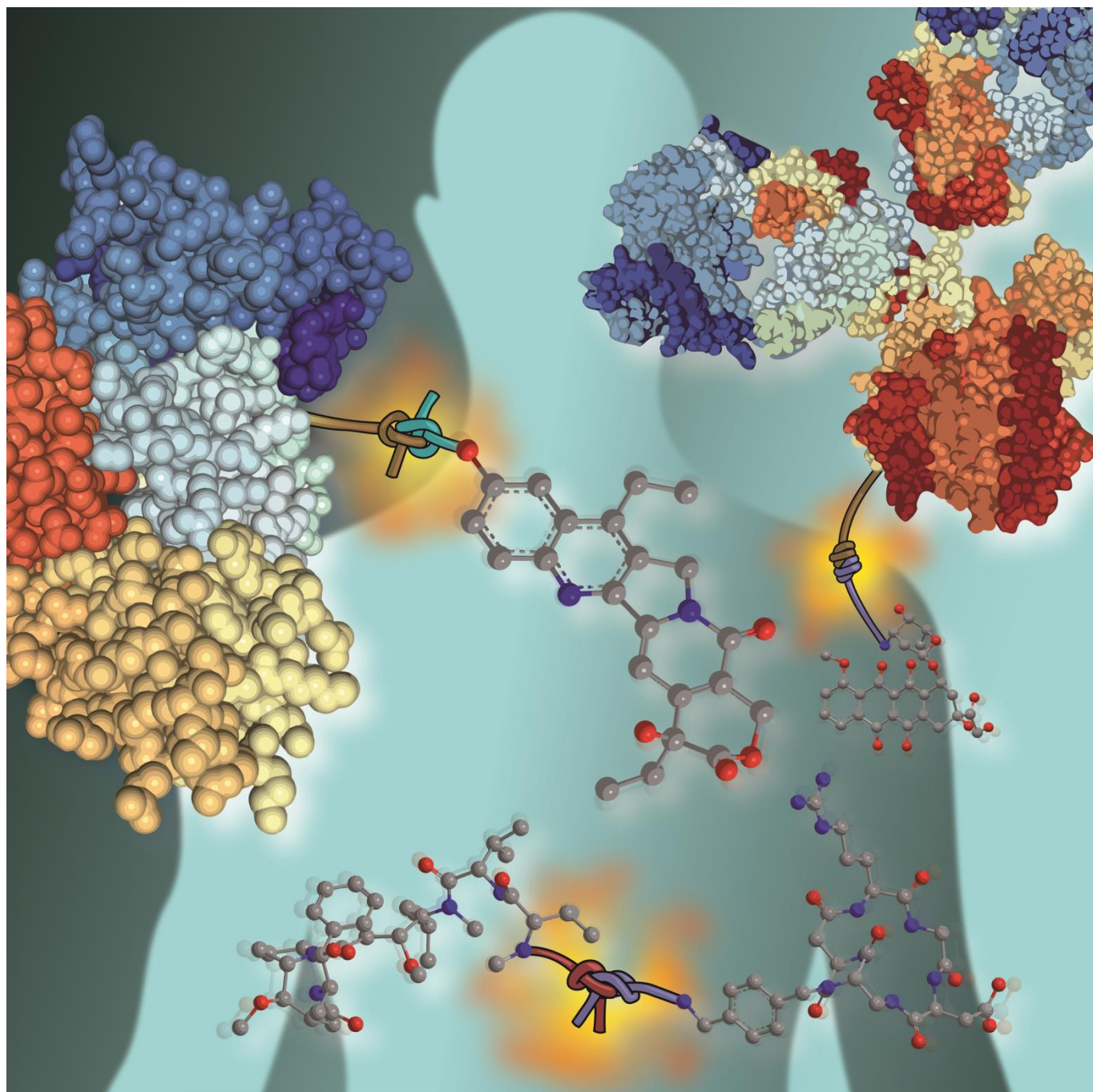


# Innovative linker strategies for tumor-targeted drug conjugates

Alberto Dal Corso,\* Luca Pignataro, Laura Belvisi and Cesare Gennari\*



**Abstract:** The covalent conjugation of potent cytotoxic agents to either macromolecular carriers or small-molecules represents a well-known approach to increase the therapeutic index of these drugs, thus improving treatment efficacy and minimizing side-effects. In general, cytotoxic activity is displayed only upon cleavage of a specific chemical bond (linker) which connects the drug to the carrier. The perfect balance between the linker stability and its selective cleavage represents the key for success in these therapeutic approaches and the chemical toolbox to reach this goal is continuously expanding. In this review, we highlight recent advances on the different modalities to promote the selective release of cytotoxic agents, either exploiting specific hallmarks of the tumor microenvironment (e.g. pH, enzyme expression) or by the application of external triggers (e.g. light and bioorthogonal reactions).

## 1. Introduction

The systemic administration of cytotoxic agents to cancer patients often leads to severe side effects and limits the dose escalation to therapeutically-active regimens. Despite these pitfalls, small-molecule anticancer drugs are still used to treat several kinds of early-stage or advanced tumors, administered either as single agents or in combination with radiation, before or after surgical intervention.<sup>[1]</sup> Moreover, the therapeutic outcome of modern treatment modalities, e.g. the anticancer immunotherapy, can be significantly improved by combination with specific cytotoxic agents. Indeed, the cell stress induced by anticancer agents can augment the immunogenicity of tumor cells by different pathways. Among these, the induction of immunogenic cell death (ICD) consists in the expression of damage-associated molecular patterns (DAMPs) on the surface of cancer cells, followed by the stimulation of anticancer immune responses.<sup>[2]</sup> The opportunity to improve the pharmacological effects of cytotoxic agents with a concomitant decrease of systemic toxicity has been investigated for decades, mainly through the development of different tumor-targeted prodrugs, capable of enhancing the drug accumulation at the tumor site. In a large part of these therapeutics, the bioactive molecule is covalently conjugated to a support (carrier), and it is therapeutically active only when the chemical bond (linker) between the carrier and the drug is cleaved (Figure 1). The structural assembly of the linker-drug module with the carrier accounts for the stability and activity of the construct, and a variety of conjugation strategies have been proposed and reviewed recently.<sup>[3]</sup> This review illustrates all advances in the linker technology aimed at the selective release of therapeutics and imaging agents at the tumor site, upon endogenous or external stimuli.

### 1.1. Carrier + Drug + Linker

In general, the specific drug incorporated in the tumor-targeting construct is the main effector of therapeutic activity, which can be tuned by using drugs with different potency or mode of action

(e.g. tubulin binders or DNA-damaging agents), as well as by modifying the drug loading onto the carrier. The drug's physico-chemical properties also impact on the construct activity: lipophilic payloads diffuse rapidly through the cell membrane, enabling widespread cell killing through the so-called "bystander effect",<sup>[4]</sup> whereas hydrophilic drugs often show low off-target toxicities.<sup>[5]</sup> Noteworthy, while this research field has historically found widespread application in oncology (due to the medical need for potent cytotoxic agents with improved therapeutic indexes), the preparation of targeted formulations and conjugates have also been recently proposed for other indications, such as bacterial infections,<sup>[6]</sup> osteoporosis,<sup>[7]</sup> bone fractures,<sup>[8]</sup> rheumatoid arthritis<sup>[9]</sup> and other inflammatory diseases.<sup>[10]</sup>

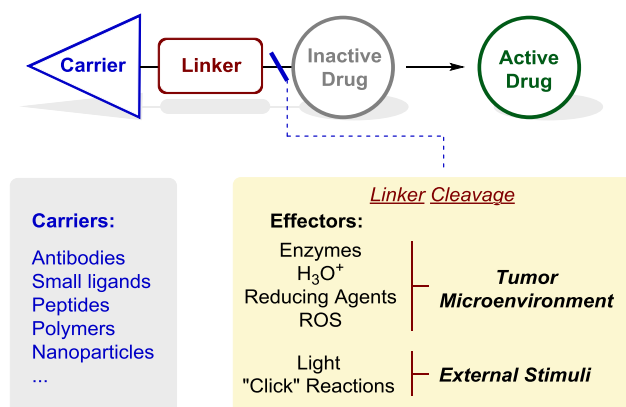


**Figure 1.** Schematic representation of tumor-targeted prodrugs, where pharmaceutical ingredients (Drug) are inactivated by covalent connection to a carrier through a specific Linker. This review surveys recent strategies for prodrug activation exploiting well-known hallmarks of the tumor environment as well as the application of external triggers.

Among the structural components of tumor-targeting devices, the carrier is the key regulator of the pharmacokinetic properties, since its size and structural features modulate the circulatory half-life, extravasation rates, residence time in the tumor and excretion. Nano-sized materials such as engineered therapeutic nanoparticles,<sup>[11]</sup> and polymer-drug conjugates (PDCs)<sup>[12]</sup> often show a preferential accumulation in tumors by "passive targeting", extravasating through the leaky tumor vasculature and persisting in the tumor owing to the altered lymphatic drainage (the so-called enhanced permeability and retention effect, EPR). Moreover, the drug conjugation to serum albumin is known to both extend its circulatory half-life and to enhance its accumulation at the tumor site, owing to the abnormal albumin uptake in highly-proliferating cancer cells.<sup>[13]</sup>

The drug conjugation to specific vehicles capable of selective binding to tumor-associated antigens is often referred to as "active targeting" strategy. With 5 products currently available on the market, antibody-drug conjugates (ADCs)<sup>[14]</sup> represent the most clinically-validated technology in this field. It has been initially postulated that, in order to limit off-target toxicities, ADCs and active-targeting therapeutics should bind to transmembrane tumor antigens and release the cytotoxic cargo inside the targeted cancer cell, upon receptor-mediated endocytosis.<sup>[15]</sup> More recently, evidence of therapeutic efficacy displayed by targeted cytotoxic agents specific to non-internalizing antigens supported the hypothesis that the extracellular drug release

[a] Dr. A. Dal Corso, Prof. Dr. L. Pignataro, Prof. Dr. L. Belvisi, Prof. Dr. C. Gennari

Dipartimento di Chimica, Università degli Studi di Milano  
via C. Golgi, 19, I-20133, Milan, Italy.

Tel: +39 0250314091; Fax: +39 0250314072

E-mail: [alberto.dalcorso@unimi.it](mailto:alberto.dalcorso@unimi.it); [cesare.gennari@unimi.it](mailto:cesare.gennari@unimi.it)

---

Alberto Dal Corso studied Chemistry at Università degli Studi di Milano, where he obtained his Ph.D. in 2015 with Prof. Cesare Gennari. He then joined the group of Prof. Dario Neri at ETH Zürich as a postdoctoral fellow. After a short period in Philochem AG (CH) working as a Research Scientist, he returned to ETH in 2017 for a post-doc co-financed by Novartis Foundation for Medical-Biological Research. Since 2018 he is working at Università degli Studi di Milano as a postdoctoral fellow, with focus on the development of ligands for protein targets and the delivery of bioactive molecules at the site of disease.



Luca Pignataro studied Industrial Chemistry at Università degli Studi di Milano, where he graduated in 2003 and received his PhD in 2006 under the supervision of Prof. Franco Cozzi. In 2007 he joined the group of Prof. David Leigh at the University of Edinburgh (UK) as a post-doc, then he returned to Italy (2008) for post-doctoral experiences in the groups of Prof. Cesare Gennari (Università degli Studi di Milano) and Prof. Umberto Piarulli (Università degli Studi dell'Insubria, Como). In 2012 he became a researcher at Università degli Studi di Milano and in 2019 he was appointed associate professor. His main research interests include synthetic methodologies, supramolecular catalysis and medicinal chemistry.



Laura Belvisi graduated in Chemistry cum laude at Università degli Studi di Milano in 1990 and received her PhD in 1994 with Prof. Carlo Scolastico. After a post-doc, she became researcher at Università degli Studi di Milano in 1998 and associate professor of organic chemistry in 2015. Between 2001 and 2011 she directed the Molecular Modeling Laboratory at the Interdepartmental Center for Bio-Molecular Studies and Industrial Applications of Università degli Studi di Milano.



Her research interests focus on peptidomimetic modulators of protein-protein interactions and the design of small integrin ligands as angiogenesis inhibitors as well as vehicles for the targeted delivery of bioactive molecules for tumor imaging and therapy.

Cesare Gennari graduated in Chemistry cum laude at Università degli Studi di Milano in 1975. After becoming an assistant professor at the same University in the group of Prof. Carlo Scolastico (1978), he joined Prof. Clark Still's group at Columbia University (NY) as a research associate (1982-1983). In 1985 he became an associate professor and in 1994 a full professor of organic chemistry at Università degli Studi di Milano. His awards include a NATO senior fellowship (1985), the Federchimica prize (1993), the Ziegler-Natta award and lecture (German & Italian Chemical Societies, 1997), the Ciamician medal (1986), the "Prize for research in synthetic organic chemistry" (2006), the Quilico (2013) and the Piria (2017) gold medals of the Italian Chemical Society. He is presently a member of the International Advisory Board of *EurJOC* and a *ChemPubSoc Europe* Fellow. His research interests include the synthesis and biomedical applications of tumor targeting peptidomimetics and conjugates.



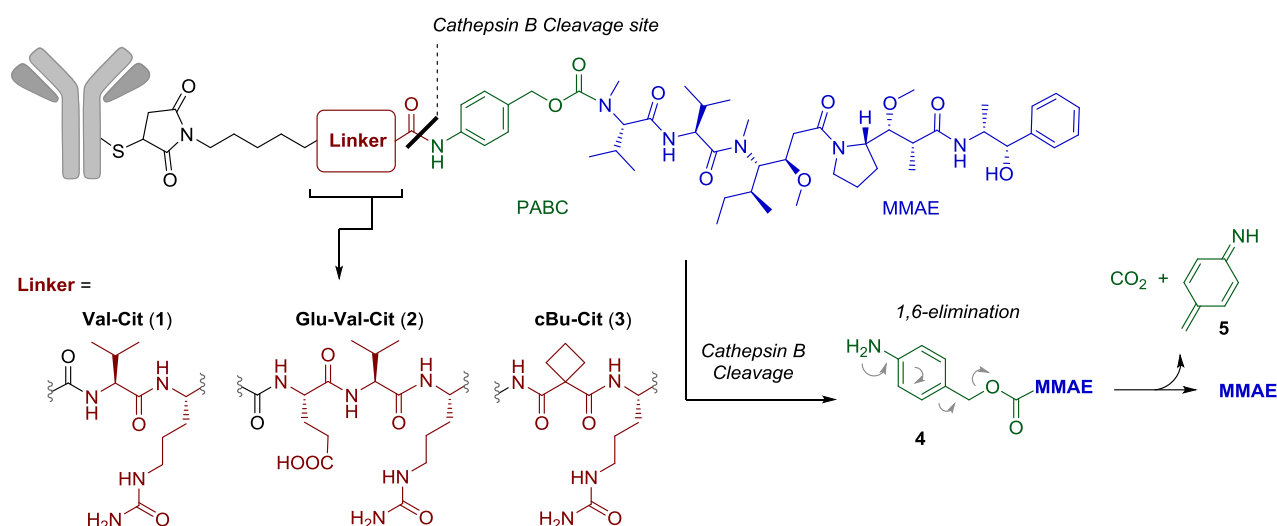
and its passive diffusion within the tumor microenvironment may also increase the treatment efficacy.<sup>[16]</sup> The clinical success of ADCs stimulated the investigation of other classes of active targeting biotherapeutics, such as antibody-conjugated nanoparticles,<sup>[17]</sup> antibody fragment-drug conjugates,<sup>[18]</sup> aptamer-drug conjugates,<sup>[19]</sup> and small molecule/peptide-drug conjugates,<sup>[20]</sup> capable of binding to tumor-associated receptors. Besides the drug and carrier moieties, the linker is the third fundamental structure, being responsible for both the stability of the intact construct in the blood stream and for the drug release at the diseased site. In particular, structural weaknesses of the linker moiety can be responsible for the low stability of the construct in circulation, resulting in premature drug release from the vehicle and suboptimal therapeutic efficacy. Moreover, chemical modifications at the linker may improve the physical chemical properties of the whole conjugate (e.g. aqueous solubility), generating homogeneous products and minimizing aggregate formation. Finally, linkers can be tailored to fully control the drug release at the tumor site. Specific linkers have been designed and developed to release payloads in the presence of specific hallmarks of cancer (e.g. acidic pH, abnormal enzyme expression, hypoxic and reducing conditions, altered expression of reactive oxygen species "ROS", etc.) and researchers are continuously upgrading the state-of-the-art in drug release, alongside with the increasing understanding of cancer biology. More recently, chemical tools for the activation of bioactive molecules in response to exogenous stimuli have also been investigated as prodrug activators. All these advances in the linker technology are paving the way to next-generation therapeutics and they will be discussed in the following Paragraphs.

## 2. Exploiting Hallmarks of Cancer: Linker Cleavage Promoted by Endogenous Stimuli

### 2.1. Enzyme-Activable Linkers

A large subset of targeted therapeutics features specific peptide sequences or carbohydrate moieties as linkers, which can be cleaved by tumor-associated enzymes. In general, this design imparts remarkable stability in serum, thus minimizing non-specific payload release also from long-circulating carriers, such as antibodies and other formulations. So far, intracellular proteases (e.g. cathepsins,<sup>[21]</sup> legumain<sup>[22]</sup>) and glycosidases ( $\beta$ -glucuronidase,<sup>[23]</sup>  $\beta$ -galactosidase<sup>[24]</sup>) have been investigated more extensively, and the cathepsin B-sensitive Val-Cit dipeptide (**1**, Scheme 1) can be considered a milestone, being included in the marketed conjugates Adcetris<sup>TM</sup> and Polivy<sup>TM</sup>, as well as in other ADCs undergoing clinical evaluation.<sup>[25]</sup> The success of these linkers has stimulated an intense research activity, especially at the industrial level, aimed not only at increasing the serum stability and cleavage selectivity of linker substrates in the presence of a specific effector, but also at the validation of new tumor-associated enzymes as potential drug release mediators. In particular, despite the overall success of the Val-Cit linker, its circulatory stability is known to be suboptimal and premature release of the monomethyl auristatin E (MMAE) payload has been associated to peripheral neuropathy and neutropenia in cancer patients.<sup>[26]</sup>

---



**Scheme 1.** Recent evolutions in Cathepsin-B cleavable linkers for drug release from ADCs. The protease specificity of the traditional Val-Cit linker (1) has been modulated by inclusion of an additional glutamic acid residue at the Val N terminus (i.e. Glu-Val-Cit linker 2, a poor substrate for mouse plasma enzyme Ces1C)<sup>[28]</sup> or by the development of peptidomimetic cBu-Cit linker 3,<sup>[30]</sup> showing enhanced specificity for cathepsin B. The drug release mechanism of the *para*-aminobenzyl carbamate spacer (PABC, in green) is also shown, where enzymatic cleavage at the linker's C terminus results in the formation of an aniline metabolite 4, which is rapidly converted to the aza-quinone-methide 5 and the free payload (monomethyl auristatin E).

Researchers at Pfizer provided evidence that mouse carboxylesterase 1C (Ces1C) may be responsible for the low Val-Cit stability in rodent serum, thus threatening the pre-clinical development of ADCs.<sup>[27]</sup> Modifications at the linker N terminus were found to efficiently modulate the substrate's specificity towards Ces1C, without affecting the drug release kinetics in the presence of cathepsin B. This evidence led to the identification of the Glu-Val-Cit linker (2, Scheme 1), where the presence of a glutamic acid residue imparts high plasma stability. In tumor therapy experiments with ADCs *in vivo*, this new linker displayed superior therapeutic activity than the traditional Val-Cit, even when the linker was further exposed to enzymatic degradation by insertion of a PEG spacer between the linker and the mAb structure.<sup>[28]</sup> While the Glu-Val-Cit linker represents a successful example of improved drug release specificity by hindering the enzymatic action of competitor enzymes, another logical strategy is to exploit available crystallographic data to tailor the linker structure and enhance the specificity towards the enzyme of interest.<sup>[29]</sup> This goal was recently pursued by Genentech, with the replacement of the Val residue in the Val-Cit dipeptide with a cyclobutane-1,1-dicarboxamide moiety (i.e. cBu-Cit linker 3, Scheme 1).<sup>[30]</sup> When incorporated in ADCs, this peptidomimetic linker showed similar stability in circulation but higher cathepsin B specificity than the Val-Cit standard, enabling superior therapeutic performances in tumor-bearing mice. In recent years, new enzymes have been identified as suitable effectors of linker cleavage from drug delivery vehicles. Among these, caspase 3 is an intracellular protease involved in the apoptotic pathway. Under stress conditions, this pro-enzyme is activated by the apoptosis initiator caspase 9 and its proteolytic activity in the mitochondria contributes to the interruption of ATP synthesis.<sup>[31]</sup> Due to its substrate specificity, the Asp-Glu-Val-Asp linker (DEVD) sequence has been recently used as caspase 3-cleavable linker in different therapeutic or diagnostic constructs. Similarly to cathepsin B-cleavable dipeptides, the DEVD sequence is cleaved at its C terminus and this moiety can be efficiently conjugated to various payloads through the well-known *para*-aminobenzyl carbamate spacer (PABC, as shown in Scheme 1). Interestingly, prodrugs featuring the DEVD linker (e.g. conjugate AP1-DEVD-DOX 6, in Figure 2) have been often

administered to tumor-bearing mice in combination with radiotherapy, which is important to initiate the apoptotic cascade and caspase 3 activation: this combined treatment resulted in a higher extent of apoptotic cells, thus improving the therapeutic outcomes.<sup>[32]</sup> More recently, the DEVD linker was installed in a caspase 3-activable photoacoustic probe, which enabled high-resolution imaging of tumor apoptosis in response to chemotherapy.<sup>[33]</sup> While caspase 3 has been only recently investigated for drug delivery purposes, the functionalization of anticancer agents with peptide substrates of lysosomal endopeptidase legumain has been extensively described in the literature. However, in a recent publication, researchers at Bayer reported the use of legumain-sensitive linkers for the design of a so-called antibody-prodrug conjugate (APDC).<sup>[34]</sup> The latter compound (BAY-356-KSPi-AaN, 7 in Figure 2) was composed by a kinesin spindle protein inhibitor (KSPi) payload, connected to a mAb (specific to the transmembrane TWEAK receptor)<sup>[35]</sup> via a non-cleavable linker, capable of releasing the payload only upon receptor-mediated endocytosis and lysosomal degradation of the whole antibody structure. Since uptake of the employed antibody was found to occur also in healthy organs (i.e. liver), Lerchen and coworkers connected legumain-cleavable peptides to the payload. This APDC design aimed at enhancing the specific drug activation in tumor cells, mediated by the abnormal expression of intracellular protease. This approach proved successful, as the payload protection with the legumain-cleavable linker resulted in the accumulation of free drug in tumors with higher tumor:liver ratios, compared to an analogue APDC featuring a Val-Cit cap.

While linkers cleaved by lysosomal enzymes have been mostly investigated for drug delivery purposes, it has recently become clear that cathepsin B and other primarily intracellular enzymes can be expressed also in extracellular compartments, shed by apoptotic or dead cells. Indeed, lysosomally-cleavable linkers (Val-Cit, Val-Ala, glucuronide fragments) were found to efficiently release cytotoxic payloads at the tumor site also when installed onto non-internalizing carriers, such as albumin,<sup>[36]</sup> certain monoclonal antibodies<sup>[37]</sup> and small ligands.<sup>[38]</sup> Moreover, extracellular enzymes have also been considered for the release of cytotoxic payloads from different carriers. For instance, matrix

metalloproteinases (MMPs) are calcium-dependent endopeptidases which require coordination of a zinc ion to mediate catalysis. A large part of MMPs are either anchored to the cell membrane or secreted in the extracellular milieu, where they degrade a broad range of ECM proteins (especially all collagen types, including gelatin). Owing to this large substrate diversity, MMPs play key roles in every biological process involving ECM remodeling. Nearly all members of the MMP family have been found to be dysregulated in human cancers, where they promote cancer invasion and metastasis.<sup>[39]</sup> For this reason, collagen-like peptide sequences such as Pro-Leu-Gly (PLG) have been exploited as cleavable linkers.<sup>[40]</sup> In particular, the latter have found widespread application in particulate drug delivery systems (e.g. micelles, liposomes or nanoparticles) and polymeric carriers, which tend to accumulate in tumors by EPR effect and may be efficiently activated by extracellular

proteases.<sup>[41]</sup> Another extracellular enzyme that has been selected as mediator of drug release is the serine protease elastase, stored in azurophilic granules of neutrophils and released into the extracellular space in response to infections or inflammation stimuli. Several different tumors show high levels of elastase expression, and this phenotype often correlates with poor prognosis.<sup>[42]</sup> In 2002, researchers at Bayer reported the in vitro evaluation of a tumor-targeted conjugate featuring a novel elastase-cleavable linker, consisting in the Asn-Pro-Val (NPV) tripeptide.<sup>[43]</sup> Ever since this first patent, no further investigations on this linker were reported. Our group recently investigated the NPV linker as trigger for the release of paclitaxel from the peptidomimetic compound *cyclo*(DKP-RGD), a non-internalizing ligand of the tumor receptor integrin  $\alpha_v\beta_3$ .

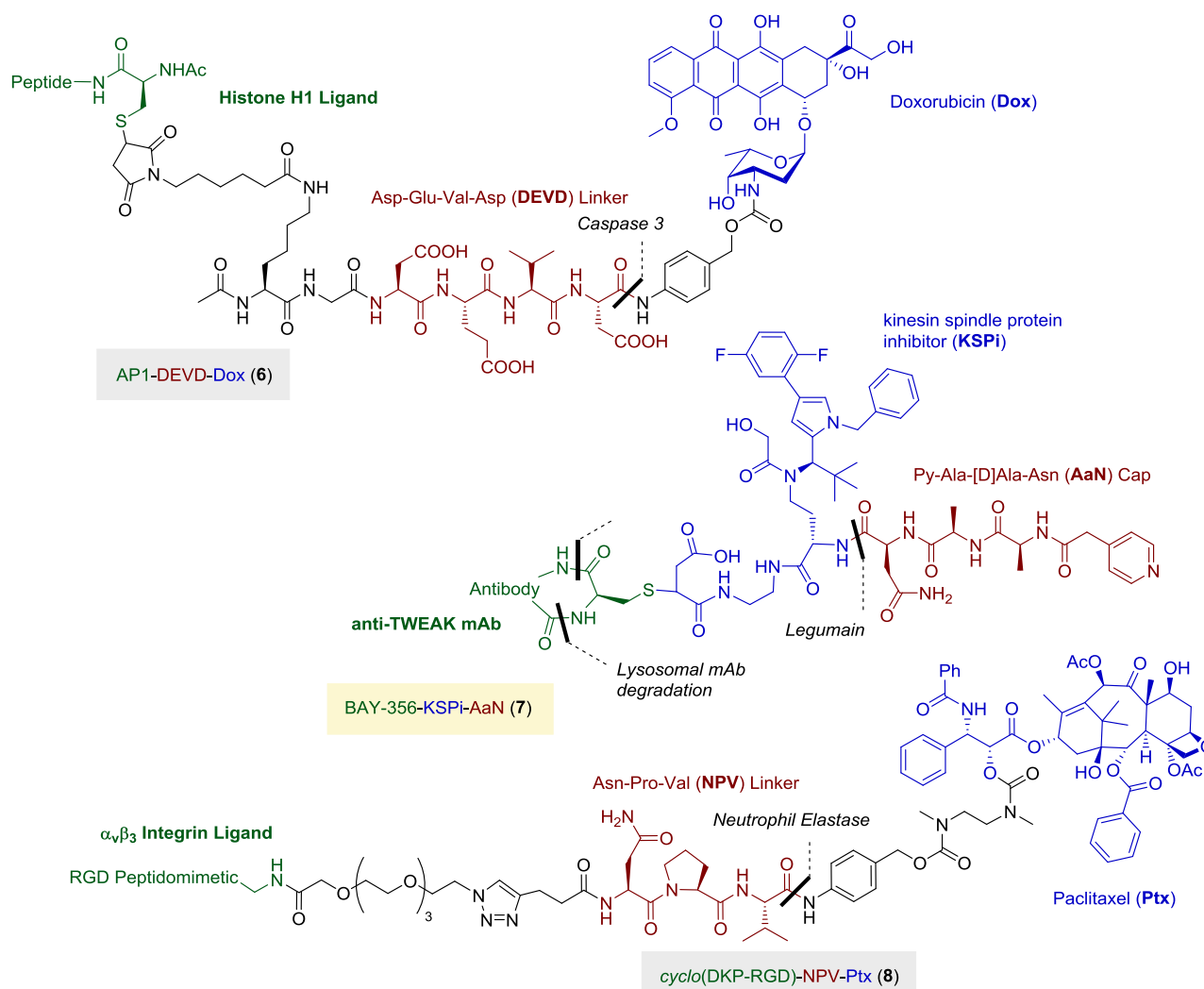


**Figure 2.** Molecular structures of peptide-drug conjugate AP1-DEVD-DOX (**6**), APDC BAY-356-KSPi-AaN (**7**) and *cyclo*(DKP-RGD)-NPV-PTX (**8**). Conjugate **6** is composed of the anticancer drug doxorubicin, the ApoPep-1 peptide (AP1, capable of binding histone H1, translocated on the cell surface of apoptotic cells) and the caspase 3-sensitive linker DEVD.<sup>[32]</sup> Conjugate **7** is composed of a mAb specific to the TWAK receptor, conjugated to a KSP inhibitor with a non-cleavable connection (antibody endocytosis leads to protein degradation and release of the drug metabolite featuring a mAb-derived Cys residue, depicted in green). A peptidomimetic legumain substrate cap Py-AaN (red) is connected to the payload and enables drug activation in the lysosomes of cancer cells.<sup>[34]</sup> Conjugate **8** features paclitaxel as payload, the  $\alpha_v\beta_3$  integrin ligand *cyclo*(DKP-RGD) and the NPV tripeptide as linker, cleavable by neutrophil elastase.<sup>[44]</sup> Cleavage site of all linkers is indicated: while doxorubicin is released from conjugate **6** with the PABC spacer elimination shown in Scheme 1, drug release mechanism of conjugate **8** is described in Scheme 5.

The resulting conjugate **8** (Figure 2) was subjected to cleavage experiments in vitro, which demonstrated that the NPV trigger is remarkably stable in mouse plasma ( $t_{1/2} = 35.3$  h) while acting as preferential substrate of purified neutrophil elastase, rather than

of a mixture of lysosomal proteases extracted by rat liver.<sup>[44]</sup> Cell viability assays showed that paclitaxel release from conjugate **8** and subsequent cytotoxic effects only occur upon addition of neutrophil elastase to the cell medium. Considering that

inflammation and the presence of infiltrating leukocytes is one of the hallmarks of cancer,<sup>[45]</sup> these data hold promises for the in vivo therapeutic activity of drug conjugates featuring the NPV linker. In summary, recent literature reports confirm that enzyme-labile linkers are still attractive tools to achieve selective drug release at the diseased site. Suitable peptide or glycoside substrates can be identified for virtually any enzyme of interest and hit-to-lead structural modifications can be introduced to further improve selectivity and chemical stability. However, significant challenges arise from the elucidation of enzyme expression (which can remarkably depend on the tumor type and development stage) and localization (e.g. lysosomal enzymes may show intracellular expression in vitro and significant stromal expression in in vivo models). Moreover, the choice of suitable carriers for therapeutic purposes have to take into account these aspects, in order to align the pharmacokinetic properties of the drug conjugate with the intrinsic properties of the effector enzyme.

## 2.2. Hydrolytically-Labile Linkers

The activation of anticancer therapeutics under acidic conditions represents a widely explored strategy for both “passive” and “active” targeting technologies. The acidification of tumor tissues derives from the inadequate oxygen delivery to fast-proliferating tumor cells, which undergo metabolism switch from the oxidative phosphorylation pathway to glycolysis. The latter is characterized by a high concentration of metabolic intermediates such as lactate and pyruvate, which sustain the high proliferation rate of cancer cells (being important for the biosynthesis of amino acids, nucleotides and lipids) and are responsible for the enhanced acidification of the extracellular milieu.<sup>[46]</sup> Moreover, acid-mediated drug release can also occur inside cancer cells, as receptor-mediated endocytic pathways are generally accompanied by a progressive acidification of the intracellular compartments.<sup>[47]</sup> The peculiar status of the tumor mass originating from the altered cell metabolism has also prompted the investigation of different types of redox-sensitive linkers, capable of releasing payloads either under reducing (e.g. disulfide linkers)<sup>[48]</sup> and hypoxic conditions (e.g. quinone and nitro/azo-arene linkers)<sup>[49]</sup> or by the presence of reactive oxygen species “ROS” in abnormal concentrations (e.g. thioketal, arylboronic ester and aryloxalate linkers)<sup>[50]</sup>; these topics have been discussed elsewhere<sup>[48-50]</sup> and will not be reviewed here. In addition to reducible linkers, a large variety of hydrolytically-labile functional groups (esters, hydrazones, etc.) have been investigated to achieve tumor-targeted release of anticancer drugs from different carriers, such as antibodies,<sup>[14a]</sup> small ligands<sup>[51]</sup> and PDCs.<sup>[12a]</sup> Recent advances in acid-sensitive prodrugs aim at maximizing the difference of linker cleavage rates between acidic and neutral pH values, enhancing the selectivity of payload release. Within this context, Wagner and coworkers measured the hydrolysis rate of several functional groups in model compounds at pH 7.4 and 5.5, and the different bonds were classified according to their selective cleavage at acidic pH compared to neutral conditions ( $t_{1/2}$  at pH 5.5 vs.  $t_{1/2}$  at pH 7.4).<sup>[52]</sup> Among the tested functional groups, the *spiro*-orthoester linker (SpiDo)<sup>[53]</sup> exhibited an optimum balance between fast cleavage rates at acidic pH and high hydrolytic stability under neutral conditions ( $t_{1/2}$  at pH 5.5  $\approx$  10 min;  $t_{1/2}$  at pH 7.4  $\approx$  2.3 h).

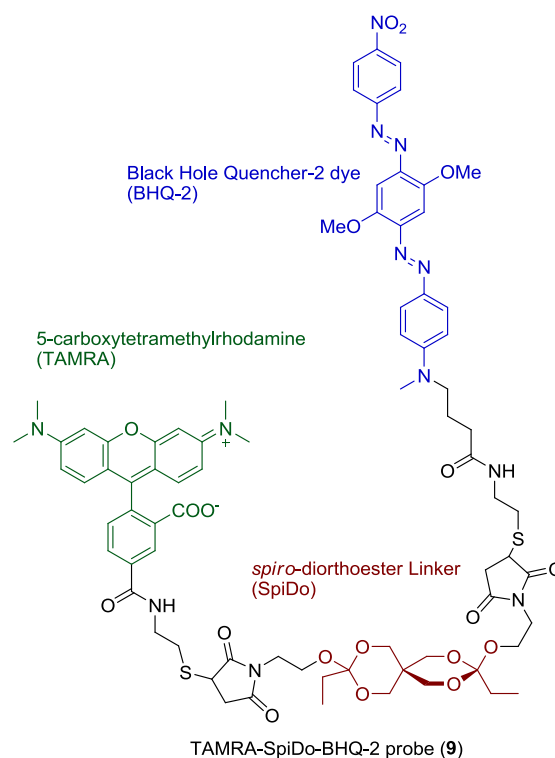
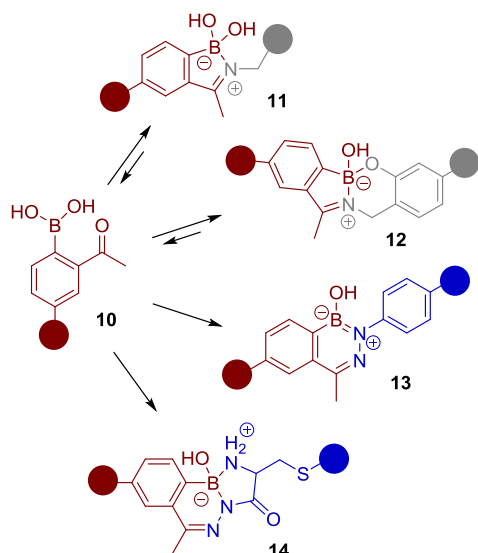


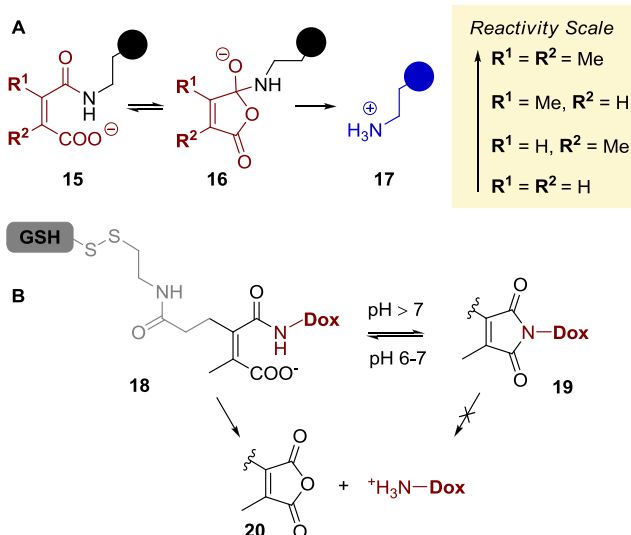
**Figure 3.** Molecular structure of the FRET probe TAMRA-SpiDo-BHQ-2 (9), featuring an acid-sensitive spiro-diorthoester linker.<sup>[52,53]</sup>

Moreover, confocal microscopy and flow cytometry experiments were performed with a FRET-based probe equipped with a *spiro*-diorthoester linker (compound 9, Figure 3): this design allowed fluorescence signal detection upon linker cleavage and the SpiDo linker showed a more selective lysosomal release in different cell lines compared to other hydrolytically-cleavable linkers (e.g. acylhydrazone, acetal, etc.).<sup>[52]</sup> Both linker reactivity and selectivity can be modulated by the introduction of specific functional groups. To this end, a first approach consists in *improving the stability of hydrolytically-labile bonds*. For instance, the hydrolytic stability of aryl imines and hydrazones can be dramatically enhanced by introducing in the *ortho*-position a boronic acid group capable of engaging a dative N-B bond (see compound 10 in Scheme 2).<sup>[54]</sup> Iminoboronates (e.g. compound 11) have been proposed as linkers for the delivery of anticancer drugs and fluorescent cargoes in the intracellular environment of cancer cells expressing the folate receptor.<sup>[55]</sup> Later on, second-generation iminoboronates have been designed to further improve the stability of standard complexes under physiological conditions. This goal was recently pursued through the generation of *N,O*-bidentate ligands, in which the iminoboronate bond is further stabilized by an additional B-O bond (e.g. compound 12 in Scheme 2).



**Scheme 2.** Stabilization of hydrolytically-labile imine and hydrazone bonds through formation of iminoboronates (**11**, **12**) and diazaborine complexes (**13**, **14**).<sup>[55b]</sup>

The resulting *N,O*-iminoboronates showed improved stability at neutral pH and in human plasma, while efficiently releasing their amine cargoes at low pH values.<sup>[56]</sup> Similarly, the reaction of *ortho*-acetyl phenylboronic acid (**10**) with carbohydrazone derivatives gives rise to a 6-membered benzodiazaborine ring (DAB, such as **13** and **14**).<sup>[57]</sup> The latter shows remarkable serum stability and hydrophilicity (due to its zwitterionic nature) and for these reasons it has been mostly exploited so far for the fast assembly of highly stable bioconjugates.<sup>[58]</sup> It is still unclear whether this functional group may also be considered as a more stable version of the traditional *N*-acylhydrazone linker,<sup>[59]</sup> with potential applications in acid-mediated release of potent hydrazone-bearing anticancer drugs.

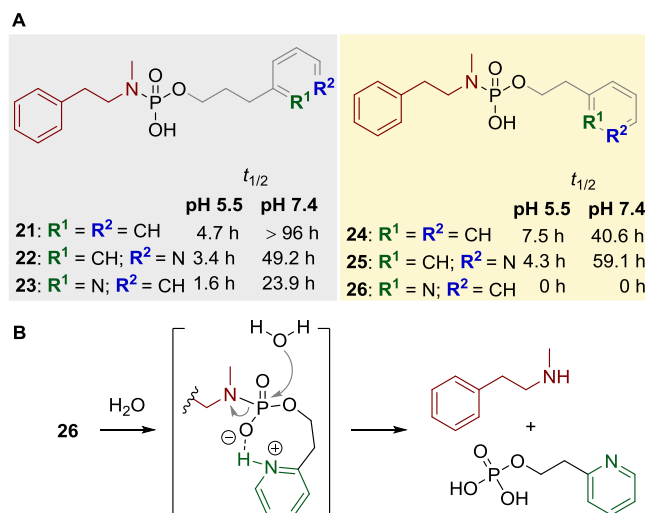


**Scheme 3.** A) Hydrolysis and substituent effects on the hydrolysis of maleamic acid derivatives.<sup>[62]</sup> B) Molecular structure of doxorubicin prodrug **18** featuring a disubstituted maleamic acid trigger and the hydrophilic glutathione (GSH) tag. While mildly acidic conditions promote drug release, hydrolysis at neutral pH competes with formation of stable imide **19**.<sup>[63]</sup>

An alternative approach consists in *making strong covalent bonds more labile to hydrolytic cleavage*. For example, while amide bonds are known to be physiologically stable and not

well-suited for payload release, mono-amides of maleic acid derivatives (e.g. compound **15** in Scheme 3) feature a proximal carboxylate group, which assists the amide hydrolysis under acidic conditions (Scheme 3 A).

The bond cleavage results in an overall charge switch (i.e. from the negatively-charged carboxylate in **15** to the positively-charged ammonium ion in **17**) and this feature has been exploited for the development of pH-responsive polymeric nanoparticles.<sup>[60]</sup> Moreover, acid-sensitive prodrugs of cytotoxic anthracycline agents have been prepared through the installation of a *cis*-aconityl linker at the daunosamine moiety.<sup>[61]</sup>



**Scheme 4.** A) Molecular structure of model phosphoramidate linkers and hydrolysis half-lives ( $t_{1/2}$ ) at pH 5.5 and 7.4. B) Proposed mechanism of intramolecularly-assisted hydrolysis of phosphoramidate linker **26**.<sup>[64]</sup>

Recently, the substituent effects on the hydrolysis rates at different pH values of maleamic acid derivatives were investigated by NMR studies. In particular, amides of 2- or 3-substituted maleic acid (derivatives of citraconic acid) underwent slower, albeit more selective acidic hydrolysis compared to the disubstituted counterparts (derivatives of dimethylmaleic acid), which proved poorly stable also at neutral pH values (Scheme 3 A).<sup>[62]</sup> On the other hand, disubstituted maleamic acid derivatives are not fully hydrolyzed at neutral pH, as the hydrolysis competes with imide formation (**19** in Scheme 3 B). For instance, An and coworkers recently developed a doxorubicin prodrug (**18**) endowed with a disubstituted maleamic acid trigger. The group showed that the equilibrium with the imide form **19** at neutral pH can inhibit doxorubicin release, whereas the fast hydrolytic cleavage results in efficient and selective drug release even at mildly acidic pH (6.5-6.9).<sup>[63]</sup>

Proximal functional groups can also promote the release of amine cargoes in phosphoramidate derivatives (Scheme 4 A). In particular, Berkman and coworkers recently reported that the introduction of H bond donors (e.g. pyridinium or carboxylic acid) at the alkoxide portion of phosphoramidate P-N bond increases the hydrolysis rate, probably due to internal H-bond assistance (Scheme 4 B).<sup>[64]</sup> This intramolecular mechanism, exhibited by pyridine-containing compounds **22**, **23**, **25**, **26** (Scheme 4 A), seems to impact more on the overall reactivity of the P-N bond towards hydrolysis rather than on the cleavage selectivity at pH 5.5 vs. pH 7.4.

In summary, the development of acid-sensitive linkers is still an attractive research area and the chemical toolbox to achieve selective drug release from a broad range of carriers is

continuously expanding. However, it is conceivable that the progress of this field will require a more systematic evaluation of stability and reactivity of these new linkers in plasma and in vivo, especially when incorporated in real therapeutic platforms rather than in model compounds.

### 2.3. Drug-Linker Connections and Self-Immolative Spacers

As discussed in the previous paragraphs, the cleavage of a specific chemical bond at the linker moiety should unmask the payload in its active form. However, the opportunity to directly connect the linker and the drug through the cleavable chemical bond are limited by structural implications (e.g. the suitable anchoring points at the drug site may not be compatible with a specific linker, steric hindrance may limit drug conjugation and linker cleavage, etc.).

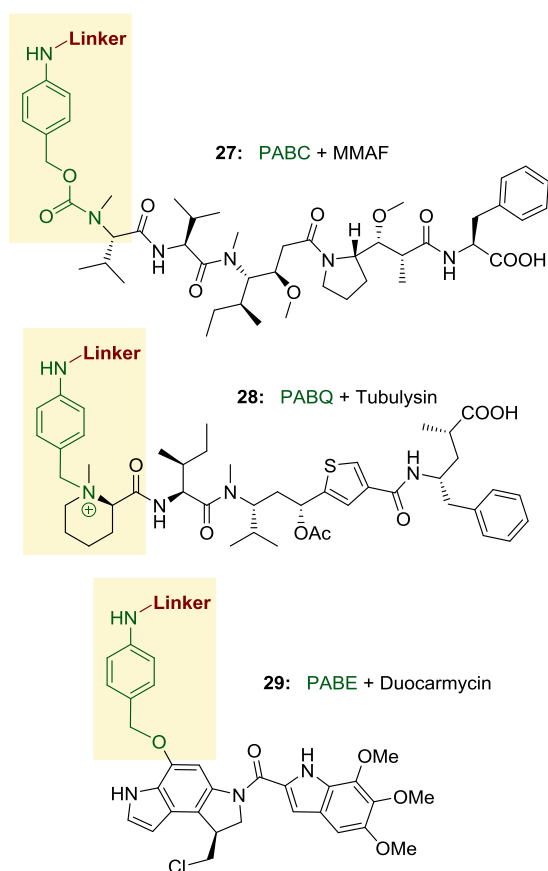


**Figure 4.** Evolution of PAB-based self-immolative spacers from the protease-promoted release of payloads bearing secondary amine (e.g. MMAF in **27**, connected through a carbamate bond, PABC),<sup>[66]</sup> tertiary amine (e.g. Tubulysin in **28**, connected through a quaternary ammonium group, PABQ),<sup>[67]</sup> and phenol group (e.g. Duocarmycin in **29**, connected through an ether bond PABE).<sup>[68]</sup>

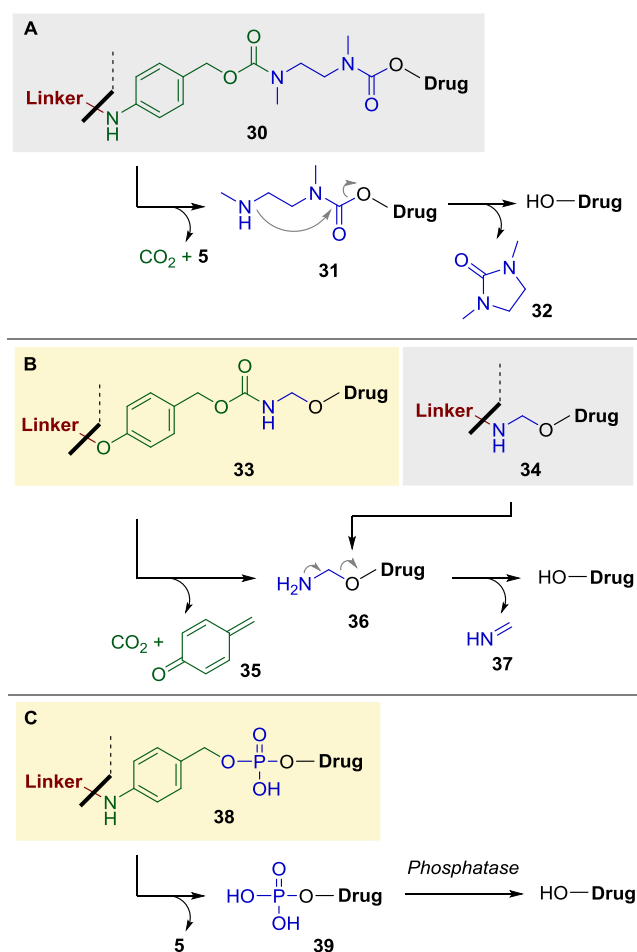
For these reasons, spacers between linker and drug fragments are often installed, either acting as chemical adaptors or to lower the steric hindrance around the cleavable bond (especially, when enzyme-sensitive cleavable linkers are used). These structures are often referred to as “self-immolative” (S.I.) spacers, as they undergo spontaneous degradation upon linker cleavage.<sup>[65]</sup> Aromatic moieties and conjugated  $\pi$ -systems represent ideal structures for the generation of self-immolative spacers and the *para*-aminobenzyl (PAB) scaffold can be considered the most versatile structure in this context. Once the free aniline moiety is disconnected from the linker, this group undergoes a fast 1,6-elimination, affording an azaquinone

methide metabolite (compound **5** in Scheme 1) and releasing different functional groups from the benzylic position (Figure 4). For instance, a large number of ADCs undergoing clinical evaluations, including the marketed Adcetris™ and Polivy™ feature a *para*-aminobenzyl carbamate (PABC) spacer, in which the release of amine-bearing drugs (e.g. MMAF in compound **27**, Figure 4)<sup>[66]</sup> takes place through the electronic cascade and loss of CO<sub>2</sub> (mechanism shown in Scheme 1).

An evolution of the traditional PABC spacer was recently presented by Genentech, with the development of the *para*-aminobenzyl quaternary ammonium salt (PABQ) spacer (compound **28** in Figure 4).<sup>[67]</sup> This is formed by converting Val-Cit-C<sub>6</sub>H<sub>4</sub>CH<sub>2</sub>OH into a the corresponding benzyl chloride Val-Cit-C<sub>6</sub>H<sub>4</sub>CH<sub>2</sub>Cl, which is then reacted with tertiary or heteroaryl amine moieties of different payloads. This feature of the PABQ spacer expands the scope of the traditional PABC, which can be used to conjugate primary and secondary amines. When incorporated in ADCs, the PABQ spacer was tested in mice, showing optimal stability in circulation and high therapeutic efficacy. The same group adopted this strategy to conjugate phenol-bearing drugs. However, the resulting *para*-aminobenzyl ether (PABE, in compound **29**) spacer showed efficient drug release rates only with payloads bearing highly acidic phenolic groups, as the presence of electron-donating groups on the phenol was found to impair the release.<sup>[68]</sup> A traditional strategy to conjugate bioactive molecules at hydroxyl groups consists in the carbamate formation between the drug and an ethylenediamine moiety, which is coupled to the PABC spacer through a second carbamate bond (compound **30** in Scheme 5 A). In this dicarbamate spacer, the drug's free OH group is released upon amine cyclization in intermediate **31** and formation of the cyclic urea **32**. Although spacer **30** has been often used to conjugate drugs bearing phenolic,<sup>[69]</sup> primary,<sup>[70]</sup> secondary<sup>[44]</sup> and tertiary<sup>[71]</sup> hydroxy groups, the amine cyclization is the rate limiting step in the drug release process, which can be further slowed down by amine protonation under acidic pH.<sup>[44]</sup> In 2016, researchers at Seattle Genetics<sup>[72]</sup> reported a methodology for the release of HO-bearing drugs based on a *N*-methylene-alkoxy group connected to a *p*-hydroxybenzyl alcohol-derived residue (compound **33** in Scheme 5 B). Although this approach had been previously reported for different applications,<sup>[73]</sup> the *N*-methylene-alkoxy spacer was first employed in the ADC area in 2016.<sup>[72]</sup> Upon cleavage of a  $\beta$ -glucuronidase-sensitive linker connected to the phenolic oxygen, compound **33** releases a hemiaminal derivative of formaldehyde (**36** in Scheme 5). The latter undergoes hydrolysis to give the cytotoxic payload (either free auristatin E or the camptothecin derivative SN38).<sup>[74]</sup> In the same year (2016), researchers at Daiichi Sankyo independently reported the use of the *N*-methylene-alkoxy spacer to directly connect a primary alcohol group of the topoisomerase I inhibitor DS-8201a to the C terminus of a peptide linker (compound **34** in Scheme 5 B).<sup>[75]</sup> The efficacy of both these new ADC settings was confirmed by in vivo tumor therapy experiments, which support the use of the methylene alkoxy spacer for the delivery of HO-bearing payloads. Finally, an innovative approach to connect HO-bearing drugs to linker modules was recently proposed by Merck: although self-immolative spacers aim at releasing the payload spontaneously, the group reported the use of enzyme substrates as spacers between drug and linker. In particular, the primary hydroxy group of an immunosuppressive drug (budesonide) was connected to a Val-Cit-PAB module through a phosphate or a diphosphate group (see compound **38**



in Scheme 5 C), which led to an overall increased hydrophilicity of the linker-payload module.



**Scheme 5.** Examples of common spacers used for release of HO-bearing drugs and their drug release mechanisms. A) Construct **30** contains a dicarbamate spacer based on the PABC/ethylenediamine combination. B) **33** and **34** feature a *N*-methylene-alkoxy group (in blue) coupled either to a PAB-like spacer through a carbamate bond (in **33**) or to a peptide linker through a protease-cleavable amide bond (in **34**). C) In conjugate **38** the PAB spacer is connected to a hydroxyl through a phosphate group.

Moreover, this design resulted in high plasma stability, while the release of free budesonide in rat lysosomal lysates was confirmed: upon linker cleavage mediated by cathepsin B, phosphatases efficiently release the free drug from phosphate metabolite **39**. Efficacy was confirmed by activity assays *in vitro*, as the linker-drug module incorporated in an ADC structure promoted the expression of GILZ protein (glucocorticoid-induced leucine zipper) in antigen-positive 786-O cells, as determined by RT-PCR.<sup>[76]</sup> In summary, the large amount of recent literature reports on chemical connections between drugs and linker indicates that chemists are continuously proposing new synthetic strategies to access unprecedented chemical

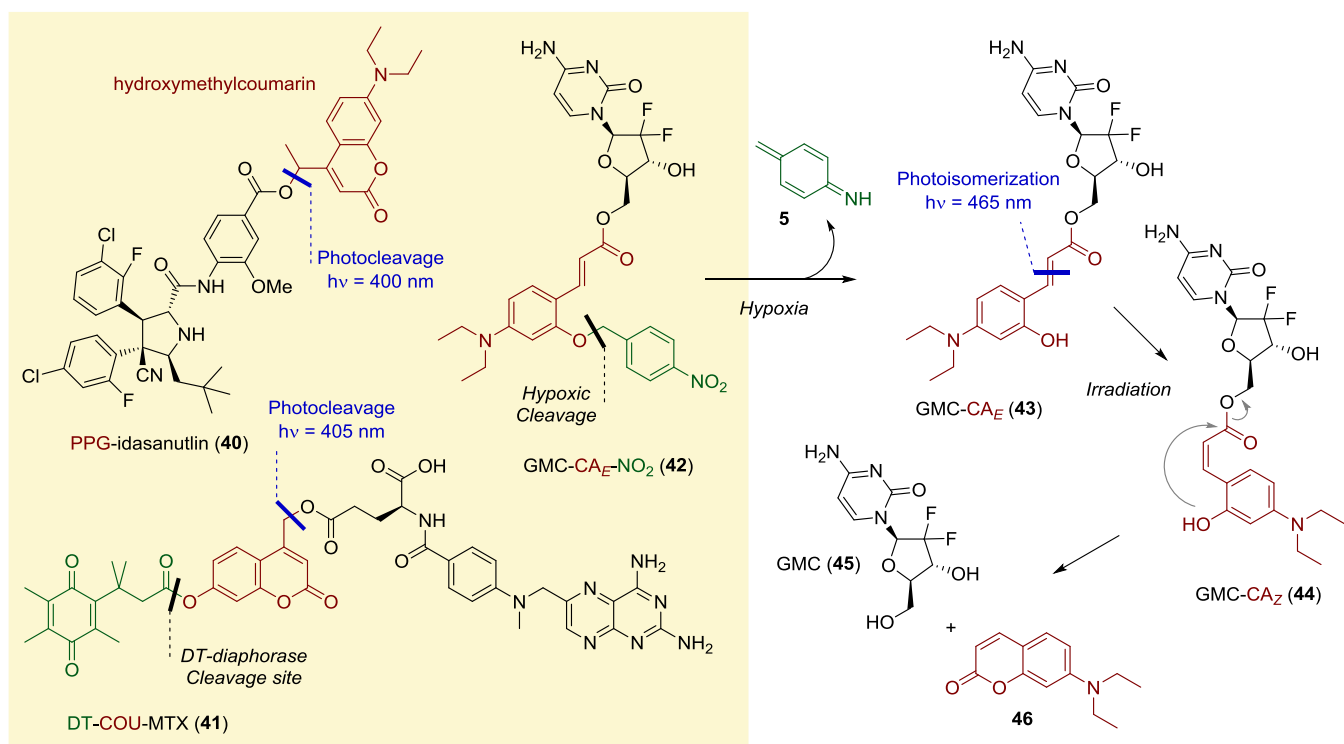
conjugations of complex bioactive molecules, as well as to overcome stability/solubility issues. Noteworthy, the significant efforts made especially by industrial groups speak for the extremely applicative flavor of these research activities.

### 3. When and Where: Linker Cleavage Promoted by External Stimuli

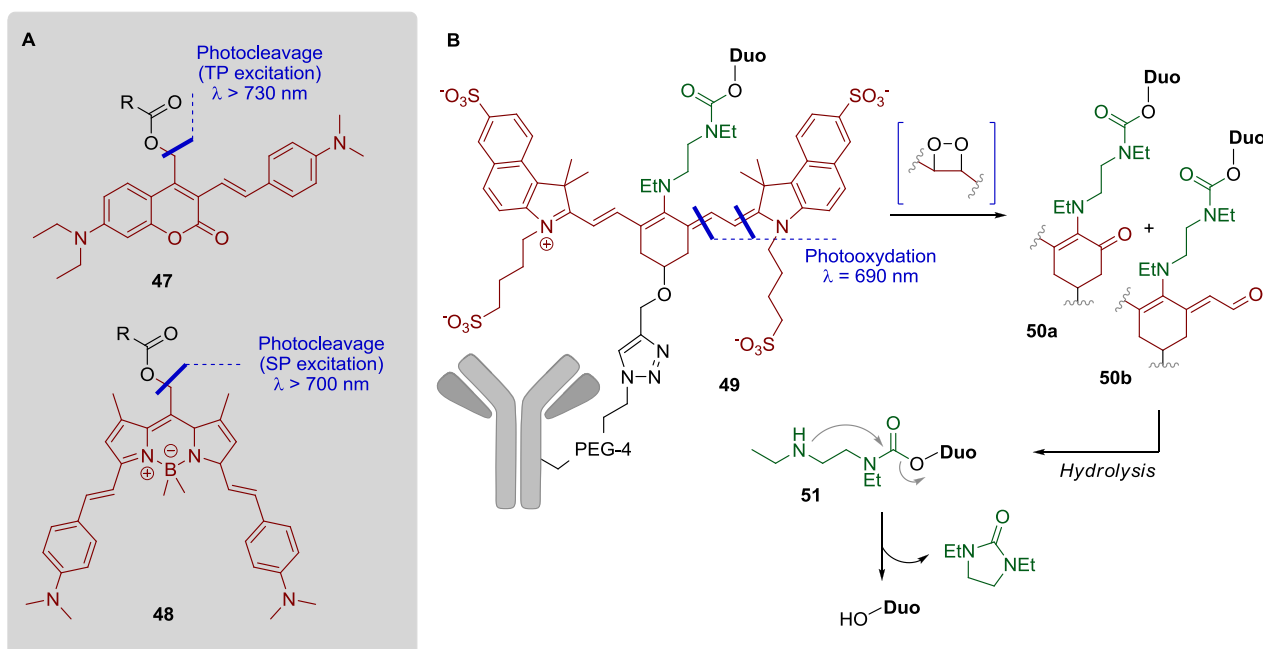
A growing body of therapeutic technologies exploit the application of external factors (i.e., other than the environmental conditions or effectors present at the tumor site) to trigger drug release from a conjugate. In the next Paragraphs, we highlight recent efforts in the development of linkers promoting drug release either upon irradiation with light or through biorthogonal reactions with a chemical trigger. These new technologies represent a revolution in the drug delivery field, holding promises for a fully controlled and “personalized” drug release, with unprecedented efficacy and tolerability profiles.

#### 3.1. UV/Vis and NIR Light- Sensitive Linkers

Light can be exploited for therapeutic purposes, using specific chemical entities capable of reacting through three different mechanisms when irradiated: cleavage of covalent bonds, isomerization, and photo-induced energy conversion.<sup>[77]</sup> In the context of drug release, a large variety of photosensitive linkers have been developed. These structures are often referred to as photolabile protecting groups (PPGs) or photocages. Owing to its high energy, UV/Vis light can induce different chemical events at the molecular level, such as covalent bond cleavage and configurational changes (e.g., double bond isomerization). Moreover, in the well-established photodynamic therapy, the irradiation of particular dyes (photosensitizers) produces cytotoxic singlet oxygen, enabling cell killing.<sup>[78]</sup> Building blocks such as *ortho*-nitrobenzyl groups, coumarinyl esters, and metal complexes have been widely used as UV/Vis light-sensitive photoremovable protecting groups.<sup>[79]</sup> Among these compound classes, coumarinyl esters represent an intensively explored class of photocages. This scaffold undergoes solvent-assisted photoheterolysis upon irradiation.<sup>[80]</sup> For instance, a visible light-sensitive coumarinyl ester was recently used by Feringa and coworkers to derivatize idasanutlin, a binder of the MDM2 protein and activator of the tumor suppressing p53 pathway (prodrug **40** in Scheme 6). As a demonstration of the high selectivity levels potentially accessible with this prodrug approach, the group performed laser irradiation of individual cancer cells, resulting in the selective drug activation at micrometer, single-cell resolution.<sup>[81]</sup> Quantum yield ( $\Phi_{rel}$ )<sup>[82]</sup> equal to 0.1% was calculated for the uncaging process of **40** upon irradiation at 400 nm by comparison with the known quantum yield for the photoreduction of a ferrioxalate solution ( $\Phi_{rel}$ : 1,14%).



**Scheme 6.** Examples of UV/Vis light activation of anticancer drugs modified with coumarin-based photocages. Solvent-assisted photocleavage of hydroxymethyl coumarin tag in compound **40** liberates free Idasanutlin, inhibitor of the MDM2-p53 protein-protein interaction.<sup>[81]</sup> Compounds **41** and **42** are two examples of pro-drugs, where the release of cytotoxic agents methotrexate (MTX) and gemcitabine (GMC) from a light-sensitive coumarin scaffold is subsequent to a preliminary activation, either mediated by tumor-associated enzymes (e.g. in compound **41** DT-diaphorase removes a quinone propionic acid moiety, depicted in green)<sup>[83]</sup> or by hypoxic conditions (e.g. nitroarene reduction and subsequent self-immolation of the resulting PABE spacer in compound **42**)<sup>[84]</sup>.



**Scheme 7.** A) Examples of  $\pi$ -extended photosensitive linkers, cleavable by either two-photon (TP, as compound **47**)<sup>[89]</sup> or single-photon (SP, compound **48**)<sup>[90]</sup> excitation with NIR wavelengths. B) ADC **49** developed by Schnermann and coworkers, based on a NIR light-sensitive cyanine linker, a duocarmycin (Duo) payload and a diamine-based self-immolative spacer (depicted in green).<sup>[94]</sup>

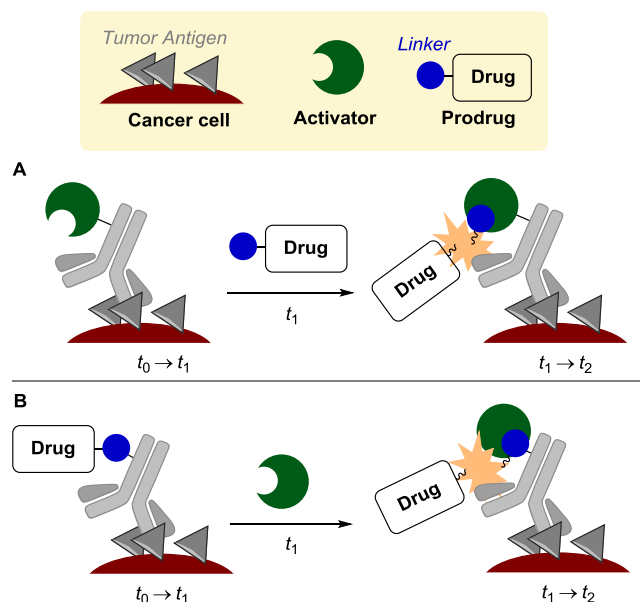
Moreover, the coumarin scaffold has been recently exploited for the generation of the so-called “pro-prodrugs”, in which drug release takes place upon combination of UV/Vis radiation and a second trigger, with the aim of improving the selectivity of drug activation. For instance, the anticancer drug methotrexate (MTX) has been recently derivatized with both a coumarin scaffold and a quinone propionic acid moiety, substrate of the reductase DT-diaphorase (pro-prodrug **41** in Scheme 6).<sup>[83]</sup> In the absence of enzyme, the quinone propionic acid moiety quenches the fluorescence of coumarin via photoinduced electron transfer (PET) and blocks the photocleavage pathway. On the contrary, MTX is released in the presence of both the enzyme and radiation. Similarly, the gemcitabine payload was masked by both a coumarin precursor and a hypoxia-sensitive nitroarene (pro-prodrug **42** in Scheme 6). Reduction of the nitro group under hypoxic conditions and UV light-induced C=C isomerization (conversion from **43** to **44**) resulted in drug release, whereas no in vitro anticancer activity was detected in the absence of one of the two stimuli.<sup>[84]</sup> Besides the double-controlled drug release, the pro-prodrugs of this class find also application as theranostic devices. Indeed, the drug release is accompanied by the release of a fluorescent coumarin derivative, allowing a direct monitoring of the drug's biological activity.

Although irradiation of the diseased site with UV/Vis light is an efficient strategy to introduce chemical modifications and to locally activate therapeutic agents, short wavelengths exhibit low tissue penetration, limiting the application of UV/Vis light to the treatment of skin, eyes or areas accessible to endoscopic techniques. Furthermore, exposure to high-energy radiation may have mutagenic effects, due to the damage of nitrogen bases in DNA strands. On the other hand, low-energy near-infrared (NIR) light (i.e.  $\lambda \approx 650\text{-}900\text{ nm}$ ) shows better safety profiles in patients and it penetrates tissues up to 10-20 mm, but it is generally too weak to cause major chemical modifications at the molecular level. For this reason, therapeutic applications of NIR light has been substantially limited to nanoscale drug delivery systems.<sup>[85]</sup> For instance, in the so-called photothermal therapy, the irradiation of suitable nanoparticles releases vibrational energy (i.e. heat), which can kill cancer cells.<sup>[86]</sup> Moreover, some nanotechnologies can upconvert NIR radiation into UV/Vis emission, a useful strategy to exploit the high tissue penetration of NIR light and the high reactivity of UV light produced in situ. This strategy has been pursued either using upconverting nanoparticles, usually lanthanide-based nanomaterials.<sup>[87]</sup> Alternatively, dyes capable of absorbing two photons of NIR light simultaneously can trigger chemical reactions similar to the one induced by a single photon of UV/visible light: this two-photon (TP) excitation can be significantly achieved in a small focal volume irradiated with a pulsed laser sources.<sup>[88]</sup> In addition to these strategies, the development of photocages capable of direct drug release when excited with red-shifted wavelengths is a field of growing interest in pharmaceutical research. This goal has been pursued so far with the generation of probes featuring extended  $\pi$ -systems, capable of undergoing electronic transitions upon irradiation with low-energy wavelengths. Also in this case, modified coumarin derivatives have been explored as NIR light-activable photocages (e.g. compound **47** in Scheme 7).<sup>[89]</sup> Moreover, Smith and Winter recently developed  $\pi$ -extended BODIPY derivatives (e.g. compound **48** in Scheme 7) featuring light absorptions above 700 nm, the longest wavelengths ever reported for photocage activation with single-photon irradiation.<sup>[90]</sup> However, since these photocages often include hydrolytically-labile ester bonds, it is not clear whether

the plasma stability may limit future translational programs. As an alternative, far-red and NIR light-promoted uncaging of anticancer drugs has been recently presented using cyanine fluorophores, which have been showing widespread application in the clinic as probes for imaging as well as in fluorescence-guided surgery practice.<sup>[91]</sup> In particular, Schnermann and coworkers developed a linker-drug module (i.e. installed onto ADC **49** in Scheme 7) capable of releasing the highly cytotoxic duocarmycin payload upon irradiation with NIR light (690 nm).<sup>[92]</sup> The proposed drug release mechanism starts with a singlet oxygen-mediated photooxidative cleavage of the cyanine polyene chain of **49** to  $\alpha,\beta$ -unsaturated carbonyl compounds (**50a,b**), occurring via dioxetane intermediates. The oxidation process increases the hydrolytic susceptibility of the enamine moiety and the released amine **51** can thus deliver the cargo (duocarmycin) upon self-immolation of an ethylenediamine spacer to give the corresponding cyclic urea (Scheme 7 B). In the absence of irradiation with NIR light, the linker-drug module showed high stability in solution ( $t_{10\%} = 230\text{ h}$ )<sup>[93]</sup>, while photorelease mechanism occurred with a half-life of 90 min. The linker-drug module conjugated to the anti-EGFR mAb panitumumab (**49**) showed promising anticancer activity in mice xenografted with MDA-MB-468 cancer cells.<sup>[94]</sup> ADC **49** was evaluated in combined therapy with a second mAb conjugated to a photoabsorber (i.e. the IR700 silicon-phthalocyanine dye), capable of causing cell swelling and cell membrane rupture upon NIR-light irradiation. In vivo therapy experiments reported the superior anticancer effects of the combination, likely due to the increased vascular permeability promoted by the photoabsorber.<sup>[95]</sup> Given the promising results shown in preclinical settings by these new classes of photoreactive probes, it is conceivable that the area of far-red and NIR light-induced drug release will experience significant development in the near future. For instance, recent reports on new scaffolds for NIR light-mediated uncaging indicate the central role of the photooxidation step, which can lead to payload release via  $\beta$ -elimination as an alternative to enamine hydrolysis.<sup>[96]</sup>

### 3.2. Pre-Targeting and “Click to Release” Strategies

The biodistribution profile of systemically-administered biotherapeutics is often suboptimal, even in the case of active-targeting technologies. For instance, it is widely accepted that large monoclonal antibodies extravasate and accumulate at the tumor site at much slower rates than small antibody fragments or small ligands.<sup>[97]</sup> On the other hand, while small therapeutics rapidly accumulate in excretory organs, large IgG mAbs often show long residency in the tumor mass and better tumor:organ and tumor:blood ratios at later time points (e.g. >24 h) from administration.<sup>[98]</sup> The so-called pre-targeting strategies aim at the drug release “on demand”, through the sequential administration of two different chemical entities, a prodrug and its activator, as chemoselective reagents (Scheme 8).



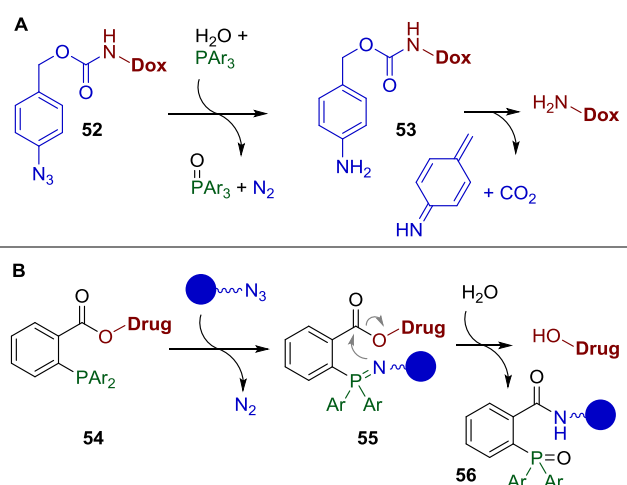
**Scheme 8.** Schematic representation of common pre-targeting strategies. A) the targeting vehicle is conjugated to an activator (e.g. an enzyme in the ADEPT technology) and accumulates in the tumor environment upon administration ( $t_0 \rightarrow t_1$ ). The prodrug is then administered (at  $t_1$ ), ideally when the targeted conjugate shows 100% selective accumulation in the tumor mass. B) the prodrug is conjugated to the targeting vehicle and administered at  $t_0$ , followed by activator dosing ( $t_1$ ) and selective drug release at the tumor site ( $t_1 \rightarrow t_2$  e.g. by means of a bioorthogonal reaction between linker and activator).

One of these entities is covalently conjugated to a tumor-targeting carrier, usually a mAb or mAb fragment and it is dosed first. This construct often shows long residence times in vivo, which implies a highly stable conjugation chemistry (half-lives in serum in the order of days). At the time point in which the first conjugate is known to reach the best biodistribution parameters in terms of tumor:organs and tumor:blood ratios (e.g.  $t_1$  in Scheme 8), the non-targeted species is administered, thus achieving an ideally 100% selective drug release at the tumor site. Unlike the targeted partner, the second construct should be small enough to exhibit efficient systemic distribution and fast clearance from tissues. For this reason, the chemical activation between the two partners should occur within minutes at low  $\mu\text{M}$  concentrations.

The pre-targeting concept was firstly elaborated in the 1990s, with the development of the antibody-directed enzyme prodrug therapy (ADEPT).<sup>[99]</sup> Here, an antibody-enzyme conjugate (i.e. the so-called catalytic antibody) binds tumor antigens on the surface of cancer cells or in the tumor interstitium and it slowly clears from blood and healthy organs (Scheme 8 A). In a second step, a prodrug is administered, whose activation is specifically carried out by the targeted catalyst, rather than by endogenous enzymes. In ADEPT, a single molecule of the targeted enzyme can catalyze the activation of several molar equivalents of prodrug, potentially resulting in a high concentration of active drug at the tumor site. Although ADEPT showed promising results in different clinical trials, the high immunogenicity of the catalytic antibody has represented a limit to its development.<sup>[100]</sup> In addition to the enzymatic activation of prodrugs, research on new bioorthogonal reactions for imaging and therapy is gaining momentum. Importantly, the bioavailability of both the targeted and non-targeted reaction partners are limited by the receptor copy number and by the rapid clearance, respectively. For this reason, to achieve optimal activity in vivo with non-toxic doses,

prodrug and activator must react rapidly (rate constants higher than  $10^{-1} \text{ M}^{-1} \text{ s}^{-1}$  are generally pursued).<sup>[101]</sup>

The Staudinger reduction ( $k \approx 10^{-3} \text{ M}^{-1} \text{ s}^{-1}$ ) has been initially proposed as a potential bioorthogonal reaction for prodrug activation. This reaction involves a phosphine and an organic azide, yielding an aza-ylide intermediate, which releases the corresponding phosphine oxide and a primary amine moiety upon hydrolysis. In a proof of concept work of 2008, Robillard and co-workers demonstrated that the presence of a molar excess of phosphine reductant in the cell medium results in the efficient activation of an azido-doxorubicin prodrug (compound **52** in Scheme 9), with subsequent cytotoxicity in vitro.<sup>[102]</sup> Later on, it was demonstrated that an ester group in the *ortho*-position of the aryl phosphine (i.e. compound **54**) can be subjected to the nucleophilic attack by an aza-ylide (see intermediate **55**). This intramolecular reaction results in the release of a HO-bearing payload, with the formation of a stable amide bond (Staudinger-Bertozzi ligation, compound **56**).<sup>[103]</sup>

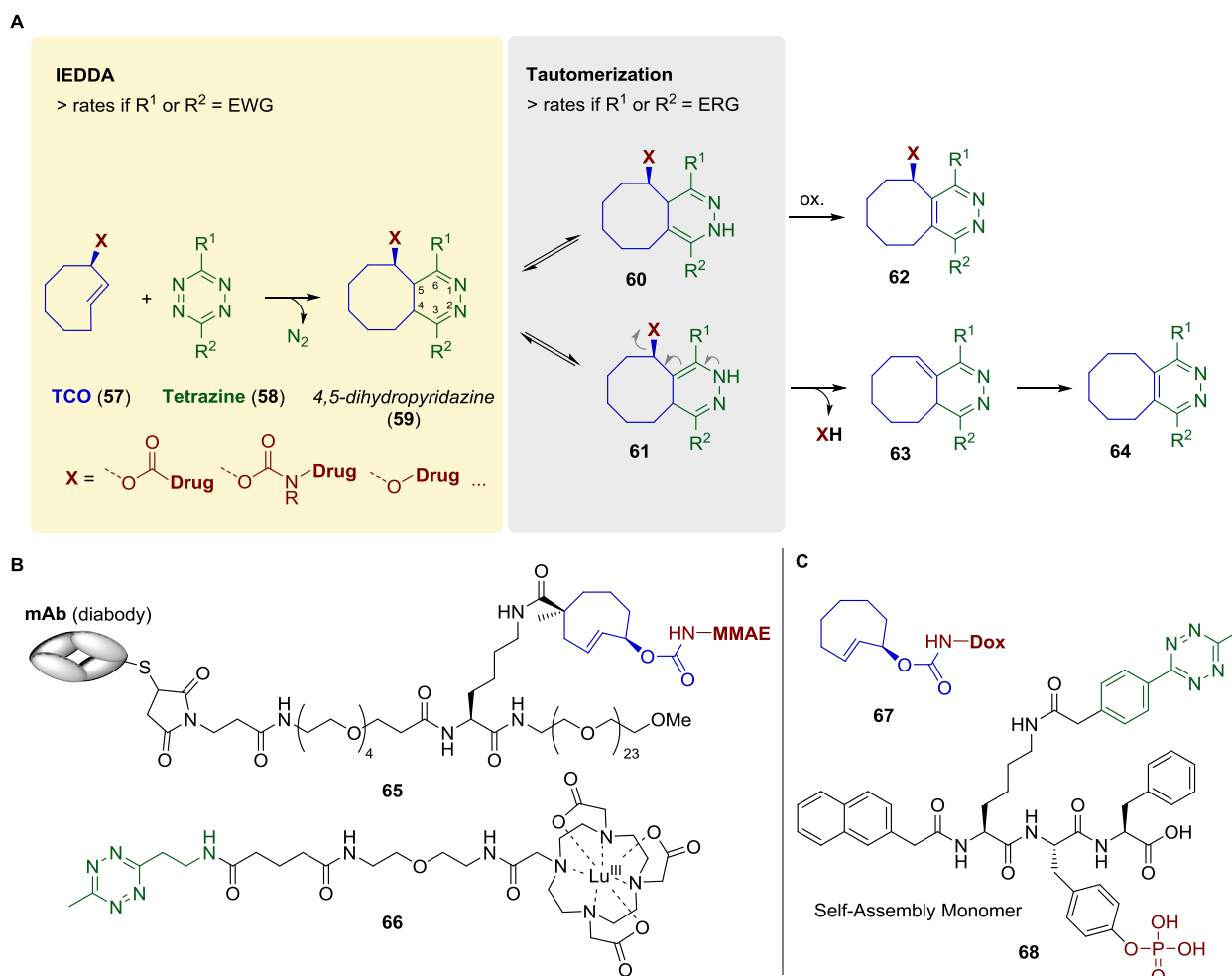


**Scheme 9.** Applications of the Staudinger reduction for prodrug activation: A) phosphine-mediated release of doxorubicin from the azide-based prodrug **52**;<sup>[102]</sup> B) Reaction mechanism of the Staudinger-Bertozzi ligation.<sup>[103]</sup>

Showing much faster kinetics than the Staudinger reaction, a series of strain-promoted cycloadditions have been proposed as suitable bioorthogonal “click” reactions, finding widespread application in chemical biology, imaging and therapy.<sup>[104]</sup> In particular, the strain-promoted alkyne-azide cycloaddition (SPAAC,  $k \approx 10^{-1}/10^0 \text{ M}^{-1} \text{ s}^{-1}$ ) and the inverse-electron-demand Diels-Alder (IEDDA,  $k$  up to  $10^5 \text{ M}^{-1} \text{ s}^{-1}$ ) conjugation between tetrazine derivatives and dienophiles (e.g. bicyclononyne, cyclopropane and *trans*-cyclooctene) provide highly stable chemical conjugations, a major requirement for imaging techniques with radioisotopes or fluorescent probes.<sup>[105]</sup> Structural modifications at both the diene and dienophile moieties have been proposed to modulate the in vivo stability of the reagents and the bioconjugation efficiency.<sup>[106]</sup> However, among the large variety of diene and dienophile partners that have been described, only a few offer the opportunity to undergo covalent bond cleavage upon the cycloaddition step (i.e. dissociative bioorthogonal reactions), potentially releasing a payload through the so-called “click and release” mechanism.<sup>[107]</sup> The paradigm in this field was introduced by Tagworks Pharmaceuticals and it consists in the *trans*-cyclooctene scaffold (TCO, compound **57** in Scheme 10 A) as cleavable linker, exploiting the fast click reaction with tetrazine activators (**58**).<sup>[108]</sup> The drug release mechanism was recently described in detail.<sup>[109]</sup> The crucial steps consist in the first cycloaddition to a

4,5-dihydropyridazine intermediate (**59**), followed by conversion to the 2,5- and 1,4-tautomers (compounds **60** and **61**). Among these, only the latter can undergo the subsequent electronic cascade, allowing the release of different functional groups (carbamic acids, carboxylic acids, phenols and alcohols).<sup>[110]</sup> Interestingly, fast click reaction does not necessarily lead to highly efficient drug release. In fact, the IEDDA and tautomerization steps are individually influenced by substituents at the tetrazine moiety (Scheme 10 A), and better drug release performances were shown by combination of two functional groups with opposite electron-releasing and withdrawing properties.<sup>[108]</sup> Moreover, acid catalysis was found to accelerate release rates by impacting on the post-click tautomerization. For this reason, tetrazines derivatization with proton-donor functional groups (e.g. carboxylates<sup>[110]</sup> and iminium ions<sup>[111]</sup>) can promote the formation of either the desired 1,4-tautomer **61** (accelerating drug release also at neutral pH) or the 2,5-analogue **60** (slowing down the release process), depending on the functional group orientation resulting from the IEDDA step. From the stability point of view, the TCO linker showed rapid *trans-cis*

isomerization in serum. While this deactivation pathway was ascribed to Cu(II) contained in proteins such as transcuprein and albumin, an increased steric hindrance around the TCO correlated with increased serum stability.<sup>[112]</sup> Similarly, tetrazine derivatives show variable stability in serum, which is generally increased by the presence of alkyl substituents.<sup>[113]</sup> The feasibility of the “click and release” approach with the tetrazine-TCO pair was recently demonstrated in two remarkable preclinical experiments. Tagworks Pharmaceuticals developed a mAb in diabody format specific for the tumor-associated glycoprotein-72 (TAG72) antigen: this mAb was conjugated to MMAE through a TCO linker, resulting in ADC **65** (Scheme 10 B). Unlike traditional IgG formats, the diabody mAb showed a high tumor uptake combined with a rapid blood clearance ( $t_{1/2} \approx 5$  hours). As a result, 48 h after injection in tumor-bearing mice, the injected ADC dose per gram (% ID g<sup>-1</sup>) was equal to 29%, while < 0.1% ID g<sup>-1</sup> was detected in blood and healthy organs. In addition, a radiolabeled tetrazine activator (compound **66**) was designed, which showed fast clearance from blood ( $t_{1/2} = 12$  minutes).



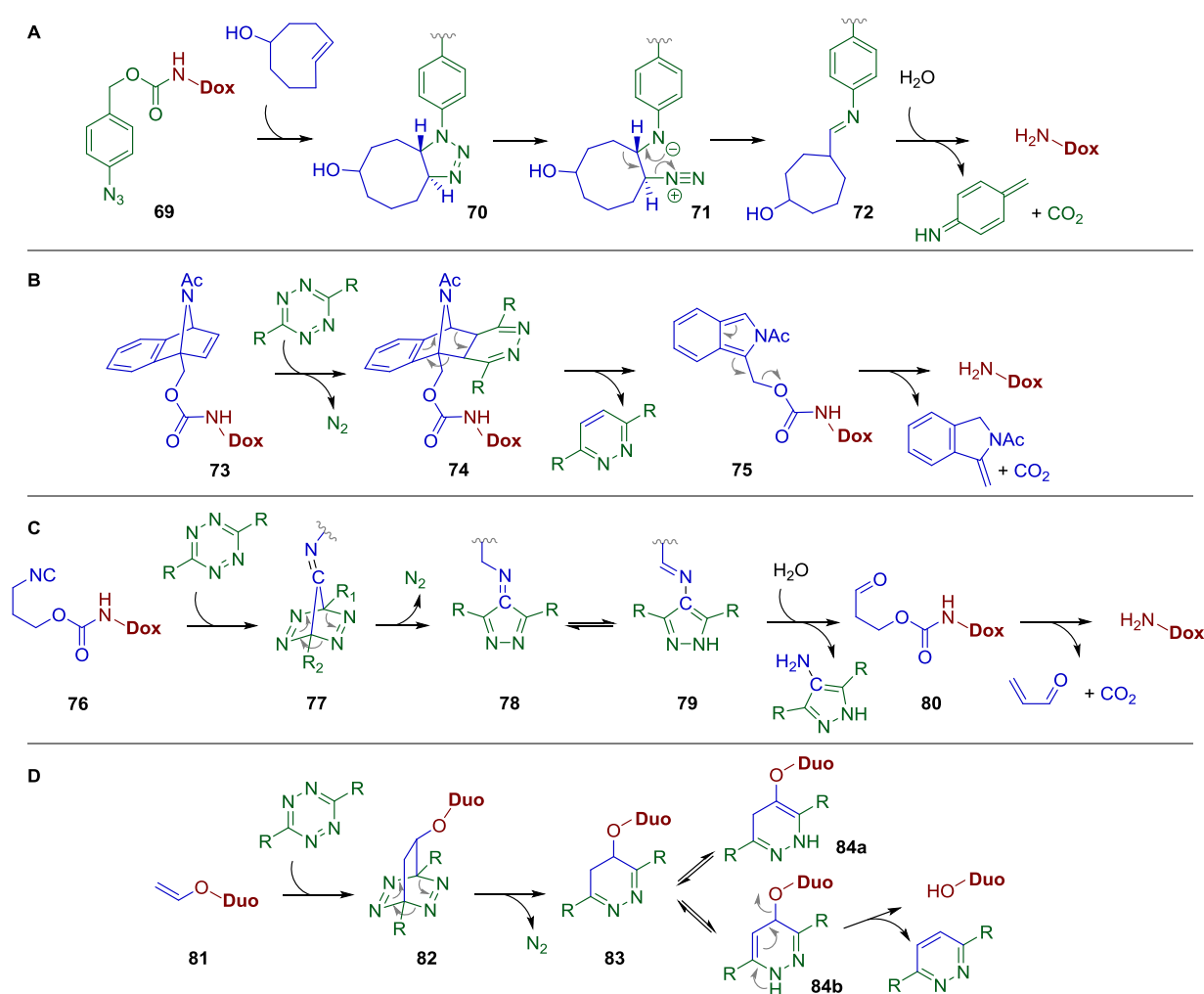
**Scheme 10.** A) Reaction mechanism of “click and release” strategy with the TCO-Tetrazine pair. Substituent effects of the fundamental IEDDA and tautomerization steps are indicated, together with the leaving groups that have been described so far.<sup>[110][111]</sup> B) Molecular structure of the TCO-Tetrazine pair used for targeted delivery of MMAE in tumor-bearing mice: the drug is connected to a monoclonal antibody in diabody format through a TCO linker (ADC **65**) and released by reaction with tetrazine **66**, 48 h post ADC injection. C) Molecular structure of the lipophilic tripeptide **68** featuring a tetrazine moiety and a *O*-Phospho-Tyr residue, whose cleavage mediated by tumor-overexpressed phosphatases promotes the tripeptide self-assembly in tumors. The enhanced tetrazine tumor retention enables the selective activation of TCO-doxorubicin prodrug **67**, administered systemically in a second step.

Treatment of tumor-bearing mice with 4 cycles of the **65-66** combination led to remarkable anticancer effects and this activity was significantly higher than the one showed by single-treatment

with an analogous MMAE-based ADC equipped with the Val-Cit linker.<sup>[114]</sup> Following a different approach, Chen, Gao and co-workers applied the “click and release” protocol with the TCO-

tetrazine pair to the tumor-targeted enzyme instructed supramolecular self-assembly (EISA) context.<sup>[115]</sup> Here, a lipophilic tripeptide (compound **68**, Scheme 10 C) featuring an O-Phospho-Tyr residue was equipped with a methyl-tetrazine moiety. Abnormal phosphatase expression in cancer cells was exploited to trigger a localized self-assembly of the tripeptide, resulting from the increased tripeptide lipophilicity upon dephosphorylation. Biodistribution analysis with <sup>125</sup>I-labelled tripeptide showed selective accumulation of the dephosphorylated compound at the tumor site as compared to plasma and liver. This effect was observed at high tripeptide doses (50 mg/Kg), which are functional to trigger a significant self-assembly in vivo. Administration of TCO-Doxorubicin prodrug **67** in tumor-bearing mice 2 hours after dosing with peptide **68** resulted in significant anticancer effects and good tolerability profile. These data hold promises for future optimization, which may enhance the tumor selectivity of the enzymatic activation and decrease the minimum effective dose. Although “click and release” approaches have been mostly pursued using the TCO/tetrazine pair, the pool of cycloaddition partners is currently expanding. Gamble and coworkers reported

the uncaging of doxorubicin upon cycloaddition reaction between an azido-PABC carbamate spacer (prodrug **69** in Scheme 11 A) and TCO, proceeding through the fast alkyl migration in a triazoline intermediate, to give nitrogen and the hydrolytically labile imine **72**.<sup>[116]</sup> With the exception of this example, a large number of dissociative bioorthogonal reactions exploit the tetrazine diene. The Franzini group reported tetrazine-mediated release of anticancer drugs from benzonornadiene cages (compound **73** in Scheme 11 B), whose high stability in serum circumvents the well-known problem of the traditional TCO scaffold deactivation through *trans/cis* isomerization.<sup>[117]</sup> In addition, the same group demonstrated that a pyrazole-imine intermediate (compound **79** in Scheme 11 C) formed by tetrazine [1+4] cycloaddition with 3-isocyanopropyl (ICP) tags (**76**) can undergo efficient payload release through imine hydrolysis and  $\beta$ -elimination in aldehyde **80**. The feasibility of this “click and release” strategy was confirmed by the efficient activation of phenolic and carbamate drugs in live zebrafish.<sup>[118]</sup>



**Scheme 11.** Reaction mechanisms of new bioorthogonal reactions for “click and release” strategies, involving reaction partners azide-TCO (A), tetrazine-benzonornadiene (B),<sup>[117]</sup> tetrazine-isonitrile (C)<sup>[118]</sup> and tetrazine-vinyl ethers (D).<sup>[119c]</sup>

Finally, the tetrazine trigger was used to release phenolic drugs caged with vinyl ether functions (compound **81**, Scheme 11 D), even though the low rates may prevent the application of tetrazine-vinyl ether pair to tumor therapy in vivo.<sup>[119]</sup>

In summary, the field of dissociative bioorthogonal reactions is expanding dramatically and the research described so far speaks for the clinical feasibility of this approach for both imaging and therapy. Hopefully, data emerging from the first

clinical investigations of these pre-targeting protocols will soon orient future development at the chemical level.

## 4. Conclusions

The selective release of pharmaceuticals at the diseased site represents a promising strategy for the treatment of cancer and other indications, following Paul Ehrlich's "Magicbullet" vision. Within this frame, both pharmaceutical companies and academic laboratories are continuously introducing new chemical linkers, either aiming at 100% selective drug release at the tumor site or to reduce toxicities in healthy organs. Recent reports seem to indicate that the combination of cytotoxic agents and prodrugs with other treatments (e.g. immunotherapy or radiotherapy)<sup>[32,120]</sup> is currently the leading strategy to induce tumor eradication and long-lasting anticancer effects. It is conceivable that a deeper understanding of the effects of different payloads on the tumor biology (e.g. increased immunogenicity and antigenicity)<sup>[2]</sup> together with the clinical validation of optimal linker and spacer connections will give rise to highly efficient drug delivery platforms, to address urgent medical needs in oncology.

## Acknowledgements

We gratefully acknowledge Ministero dell'Università e della Ricerca (PRIN 2015 project 20157WW5EH) for financial support.

**Keywords:** Drug Delivery • Prodrugs • Antitumor Agents • Photocages • Bioorthogonal Reactions

## References

- [1] American Cancer Society, Cancer Facts & Figures 2018, American Cancer Society, Atlanta, **2018**.
- [2] a) J. Galon, D. Bruni, *Nat. Rev. Drug Discovery* **2019**, *18*, 197-218; b) H.-P. Gerber, P. Sapra, F. Loganzo, C. May, *Biochem. Pharmacol.* **2016**, *102*, 1-6.
- [3] a) E. A. Hoyt, P. M. S. D. Cal, B. L. Oliveira, G. J. L. Bernardes, *Nat. Rev. Chem.* **2019**, *3*, 147-171; b) J. M. J. M. Ravasco, H. Faustino, A. Trindade, P. M. P. Gois, *Chem. Eur. J.* **2019**, *25*, 43-59.
- [4] F. Li, K. K. Emmerton, M. Jonas, X. Zhang, J. B. Miyamoto, J. R. Setter, N. D. Nicholas, N. M. Okeley, R. P. Lyon, D. R. Benjamin, C. L. Law, *Cancer Res.* **2016**, *76*, 2710-2719.
- [5] S. O. Doronina, B. A. Mendelsohn, T. D. Bovee, C. G. Cervený, S. C. Alley, D. L. Meyer, E. Oflazoglu, B. E. Toki, R. J. Sanderson, R. F. Zabinski, A. F. Wahl, P. D. Senter, *Bioconjugate Chem.* **2006**, *17*, 114-124.
- [6] a) S. Mariathasan, M. W. Tan, *Trends Mol. Med.* **2017**, *23*, 135-149; b) X. Linghu, N. L. Segraves, I. Abramovich, N. Wong, B. Müller, N. Neubauer, S. Fantasia, S. Rieth, S. Bachmann, M. Jansen, C. G. Sowell, D. Askin, S. G. Koenig, F. Gosselin, *Chem. Eur. J.* **2018**, *24*, 2837-2840; c) F. Y. Su, S. Srinivasan, B. Lee, J. Chen, A. J. Convertine, T. E. West, D. M. Ratner, S. J. Skerrett, P. S. Stayton, *J. Controlled Release* **2018**, *287*, 1-11.
- [7] H. Xie, G. Chen, R. N. Young, *J. Med. Chem.* **2017**, *60*, 7012-7028.
- [8] M. Wang, S. Park, Y. Nam, J. Nielsen, S. A. Low, M. Srinivasarao, P. S. Low, *Bioconjugate Chem.* **2018**, *29*, 3800-3809.
- [9] H. Lee, S. H. Bhang, J. H. Lee, H. Kim, S. K. Hahn, *Bioconjugate Chem.* **2017**, *28*, 1084-1092.
- [10] P. E. Brandish, A. Palmieri, S. Antonenko, M. Beaumont, L. Benso, M. Cancilla, M. Cheng, L. Fayadat-Dilman, G. Feng, I. Figueroa, J. Firdos, R. Garbaccio, L. Garvin-Queen, D. Gately, P. Geda, C. Haines, S. Hseih, D. Hodges, J. Kern, N. Knudsen, K. Kwasnjuk, L. Liang, H. Ma, A. Manibusan, P. L. Miller, L. Y. Moy, Y. Qu, S. Shah, J. S. Shin, P. Stivers, Y. Sun, D. Tomazela, H. C. Woo, D. Zaller, S. Zhang, Y. Zhang, M. Zielstorff, *Bioconjugate Chem.* **2018**, *29*, 2357-2369.
- [11] X. Xu, W. Ho, X. Zhang, N. Bertrand, O. Farokhzad, *Trends Mol. Med.* **2015**, *4*, 223-232.
- [12] a) F. Seidi, R. I. Jenjob, D. Crespy, *Chem. Rev.* **2018**, *118*, 3965-4036; b) P. Chytil, E. Koziolová, T. Etrych, K. Ulbrich, *Macromol. Biosci.* **2018**, *18*, 1700209.
- [13] a) E. N. Hoogenboezem, C. L. Duvall, *Adv. Drug. Deliv. Rev.* **2018**, *130*, 73-89; b) L. Pes, S. D. Koester, J. P. Magnusson, S. Chercheja, F. Medda, K. Abu Ajaj, D. Rognan, S. Daum, F. I. Nollmann, J. Garcia Fernandez, P. Perez Galan, H. K. Walter, A. Warnecke, F. Kratz, *J. Controlled Release* **2019**, *296*, 81-92.
- [14] Current ADCs approved for cancer treatment are Brentuximab vedotin (Adcetris™), Trastuzumab emtansine (Kadcyla™), Gemtuzumab ozogamicin (Mylotarg™), Inotuzumab ozogamicin (Besponsa™) and Polatuzumab vedotin-piiq (Polivy™). For relevant reviews on ADCs, see: a) R. V. J. Chari, M. L. Miller, W. C. Widdison, *Angew. Chem. Int. Ed.* **2014**, *53*, 3796-3827; *Angew. Chem.* **2014**, *126*, 3872-3904; b) A. Beck, L. Goetsch, C. Dumontet, N. Corvaia, *Nat. Rev. Drug Discovery* **2017**, *16*, 315-337.
- [15] D. Schrama, R. A. Reisfeld, J. C. Becker, *Nat. Rev. Drug Discovery* **2006**, *5*, 147-159.
- [16] A. H. Staudacher, M. P. Brown, *Br. J. Cancer* **2017**, *117*, 1736-1742.
- [17] a) M. C. Johnston, C. J. Scott, *Drug Discov. Today Technol.* **2018**, *30*, 63-69; b) D. A. Richards, A. Maruani, V. Chudasama, *Chem. Sci.* **2017**, *8*, 63-77; c) F. Fay, C. J. Scott, *Immunotherapy* **2011**, *3*, 381-394.
- [18] a) D. A. Richards, *Drug Discov. Today Technol.* **2018**, *30*, 35-46; b) M. P. Deonarain, *Drug Discov. Today Technol.* **2018**, *30*, 47-53; c) K. T. Xenaki, S. Oliveira, P. M. P. van Bergen En Henegouwen, *Front. Immunol.* **2017**, *8*, 1287.
- [19] a) G. Zhu, G. Niu, X. Chen, *Bioconjugate Chem.* **2015**, *26*, 2186-2197; b) S. Kruspe, F. Mittelberger, K. Szameit, U. Hahn, *ChemMedChem* **2014**, *9*, 1998-2011; c) W. Xuan, Y. Peng, Z. Deng, T. Peng, H. Kuai, Y. Li, J. He, C. Jin, Y. Liu, R. Wang, W. Tan, *Biomaterials* **2018**, *182*, 216-226.
- [20] a) M. Srinivasarao, P. S. Low, *Chem. Rev.* **2017**, *117*, 12133-12164; b) N. Krall, J. Scheuermann, D. Neri, *Angew. Chem. Int. Ed.* **2013**, *52*, 1384-1402; *Angew. Chem.* **2013**, *125*, 1424-1443; c) M. Srinivasarao, C. V. Galliford, P. S. Low, *Nat. Rev. Drug Discovery* **2015**, *14*, 203-219.
- [21] D. Dheer, J. Nicolas, R. Shankar, *Adv. Drug Deliv. Rev.* **2019**, DOI: 10.1016/j.addr.2019.01.010.
- [22] Y. Liu, K. M. Bajjuri, C. Liu, S. C. Sinha, *Mol. Pharm.* **2012**, *9*, 168-175.
- [23] S. C. Jeffrey, J. B. Andreyka, S. X. Bernhardt, K. M. Kissler, T. Kline, J. S. Lenox, R. F. Moser, M. T. Nguyen, N. M. Okeley, I. J. Stone, X. Zhang, P. D. Senter, *Bioconjugate Chem.* **2006**, *17*, 831-840.
- [24] T. Legigan, J. Clarhaut, I. Tranoy-Opalinski, A. Monvoisin, B. Renoux, M. Thomas, A. Le Pape, S. Lerondel, S. Papot, *Angew. Chem. Int. Ed.* **2012**, *51*, 11606-11610; *Angew. Chem.* **2012**, *124*, 11774-11778.
- [25] N. Jain, S. W. Smith, S. Ghone, B. Tomczuk, *Pharm. Res.* **2015**, *32*, 3526-3540.
- [26] H. Donaghy, *mAbs* **2016**, *8*, 659-671.
- [27] M. Dorywalska, R. Dushin, L. Moine, S. E. Farias, D. Zhou, T. Navaratnam, V. Lui, A. Hasa-Moreno, M. G. Casas, T. T. Tran, K. Delaria, S. H. Liu, D. Foletti, C. J. O'Donnell, J. Pons, D. L. Shelton, A. Rajpal, P. Strop, *Mol. Cancer Ther.* **2016**, *15*, 958-970.
- [28] Y. Anami, C. M. Yamazaki, W. Xiong, X. Gui, N. Zhang, Z. An, K. Tsuchikama, *Nat. Commun.* **2018**, *9*, 2512.
- [29] J. Schmitz, E. Gilberg, R. Löser, J. Bajorath, U. Bartz, M. Gütschow, *Bioorg. Med. Chem.* **2019**, *27*, 1-15.
- [30] B. Wei, J. Gunzner-Toste, H. Yao, T. Wang, J. Wang, Z. Xu, J. Chen, J. Wai, J. Nonomiya, S. P. Tsai, J. Chuh, K. R. Kozak, Y. Liu, S. F. Yu, J. Lau, G. Li, G. D. Phillips, D. Leipold, A. Kamath, D. Su, K. Xu, C. Eigenbrot, S. Steinbacher, R. Ohri, H. Raab, L. R. Staben, G. Zhao, J. A. Flygare, T. H. Pillow, V. Verma, L. A. Masterson, P. W. Howard, B. Safina, *J. Med. Chem.* **2018**, *61*, 989-1000.

- [31] M. Redza-Dutordoir, D. A. Averill-Bates, *Biochim. Biophys. Acta* **2016**, *1863*, 2977-2992.
- [32] a) S. W. Chung, Y. S. Cho, J. U. Choi, H. R. Kim, T. H. Won, S. Y. Kim, Y. Byun, *Biomaterials* **2019**, *192*, 109-117; b) Y. S. Cho, S. W. Chung, H. R. Kim, T. H. Won, J. U. Choi, I. S. Kim, S. Y. Kim, Y. Byun, *J. Controlled Release* **2019**, *296*, 241-249.
- [33] Y. Wang, X. Hu, J. Weng, J. Li, Q. Fan, Y. Zhang, D. Ye, *Angew. Chem.* **2019**, *131*, 4940-4944, *Angew. Chem. Int. Ed.* **2019**, *58*, 4886-4890.
- [34] H. G. Lerchen, B. Stelte-Ludwig, S. Berndt, A. Sommer, L. Dietz, A. S. Rebstock, S. Johannes, L. Marx, H. Jörißen, C. Mahlert, S. Greven, *Chem. Eur. J.* **2019**, *25*, 8208-8213.
- [35] J. G. Perez, N. L. Tran, M. G. Rosenblum, C. S. Schneider, N. P. Connolly, A. J. Kim, G. F. Woodworth, J. A. Winkles, *Oncogene* **2016**, *35*, 2145-2155
- [36] B. Renoux, F. Raes, T. Legigan, E. Peraudeau, B. Eddhif, P. Pointot, I. Tranoy-Opalinski, J. Alsarraf, O. Koniev, S. Kolodych, S. Lerondel, A. Le Pape, J. Clarhautad, S. Papot, *Chem. Sci.* **2017**, *8*, 3427-3433.
- [37] a) R. Gébleux, M. Stringhini, R. Casanova, A. Soltermann, D. Neri, *Int. J. Cancer* **2017**, *140*, 1670-1679; b) A. Dal Corso, S. Cazzamalli, R. Gébleux, M. Mattarella, D. Neri, *Bioconjugate Chem.* **2017**, *28*, 1826-1833; c) A. Dal Corso, R. Gébleux, P. Murer, A. Soltermann, D. Neri, *J. Controlled Release* **2017**, *264*, 211-218.
- [38] a) P. López Rivas, C. Müller, C. Breunig, T. Hechler, A. Pahl, D. Arosio, L. Belvisi, L. Pignataro, A. Dal Corso, C. Gennari, *Org. Biomol. Chem.* **2019**, *17*, 4705-4710; b) S. Cazzamalli, A. Dal Corso, D. Neri, *Mol. Cancer Ther.* **2016**, *15*, 2926-2935.
- [39] a) J. Cathcart, A. Pulkoski-Gross, J. Cao, *Genes Dis.* **2015**, *2*, 26-34; b) K. J. Isaacson, M. Martin Jensen, N. B. Subrahmanyam, H. Ghandehari, *J. Controlled Release* **2017**, *259*, 62-75.
- [40] B. E. Turk, L. L. Huang, E. T. Piro, L. C. Cantley, *Nat. Biotechnol.* **2001**, *19*, 661-667.
- [41] a) K. Nultsch, O. Gernershaus, *Eur. J. Pharm. Biopharm.* **2018**, *131*, 189-202; b) Q. Yao, L. Kou, Y. Tu, L. Zhu, *Trends Pharmacol. Sci.* **2018**, *39*, 766-781.
- [42] I. Lerman, S. R. Hammes, *Steroids* **2018**, *133*, 96-101.
- [43] H. G. Lerchen, J. Baumgarten, A. Schoop, M. Albers, (Bayer AG), PCT/EP2002/002501, WO 2002/072151, **2002**.
- [44] A. Raposo Moreira Dias, A. Pina, A. Dean, H. G. Lerchen, M. Caruso, F. Gasparri, I. Fraietta, S. Troiani, D. Arosio, L. Belvisi, L. Pignataro, A. Dal Corso, C. Gennari, *Chem. Eur. J.* **2019**, *25*, 1696-1700.
- [45] D. Hanahan, R. A. Weinberg, *Cell* **2011**, *144*, 646-674.
- [46] D. Neri, C. T. Supuran, *Nat. Rev. Drug Discovery* **2011**, *10*, 767-777.
- [47] S. Xu, B. Z. Olenyuk, C. T. Okamoto, S. F. Hamm-Alvarez, *Adv. Drug Deliv. Rev.* **2013**, *65*, 121-138.
- [48] For relevant papers on disulfide linkers, see: a) I. R. Vlahov, C. P. Leamon, *Bioconjugate Chem.* **2012**, *23*, 1357-1369; b) L.R. Jones, E.A. Goun, R. Shinde, J.B. Rothbard, C.H. Contag, P.A. Wender, *J. Am. Chem. Soc.* **2006**, *128*, 6526-6527; c) B.A. Kellogg, L. Garrett, Y. Kovtun, K.C. Lai, B. Leece, M. Miller, G. Payne, R. Steeves, K.R. Whiteman, W. Widdison, H. Xie, R. Singh, R. V. J. Chari, J. M. Lambert, R. J. Lutz, *Bioconjugate Chem.* **2011**, *22*, 717-727; d) D. Zhang, T. H. Pillow, Y. Ma, J. D. Cruz-Chuh, K. R. Kozak, J. D. Sadowsky, G. D. Lewis Phillips, J. Guo, M. Darwish, P. Fan, J. Chen, C. He, T. Wang, H. Yao, Z. Xu, J. Chen, J. Wai, Z. Pei, C. E. Hop, S. C. Khojasteh, P.S. Dragovich, *ACS Med. Chem. Lett.* **2016**, *7*, 988-993; e) G. J. L. Bernardes, G. Casi, S. Trüssel, I. Hartmann, K. Schwager, J. Scheuermann, D. Neri, *Angew. Chem. Int. Ed.* **2012**, *51*, 941-944; *Angew. Chem.* **2012**, *124*, 965-968.
- [49] For relevant reviews on hypoxia-activated drug delivery systems, see: a) A. Sharma, J. F. Arambula, S. Koo, R. Kumar, H. Singh, J. L. Sessler, J. S. Kim, *Chem. Soc. Rev.* **2019**, *48*, 771-813; b) K. Nepali, H. Y. Lee, J. P. Liou, *J. Med. Chem.* **2019**, *62*, 2851-2893; c) Y. Zeng, J. Ma, Y. Zhan, X. Xu, Q. Zeng, J. Liang, X. Chen, *Int. J. Nanomedicine* **2018**, *13*, 6551-6574.
- [50] For relevant reviews on reactive-oxygen-species-responsive drug delivery systems, see: a) G. Saravanakumar, J. Kim, W. J. Kim, *Adv. Sci.* **2017**, *4*, 1600124; b) H. Ye, Y. Zhou, X. Liu, Y. Chen, S. Duan, R. Zhu, Y. Liu, L. Yin, *Biomacromolecules* **2019**, *20*, 2441-2463; c) B. Yang, Y. Chen, J. Shi, *Chem. Rev.* **2019**, *119*, 4881-4985.
- [51] A. Dal Corso, L. Pignataro, L. Belvisi, C. Gennari, *Curr. Top. Med. Chem.* **2016**, *16*, 314-329.
- [52] S. A. Jacques, G. Leriche, M. Mosser, M. Nothisen, C. D. Muller, J. S. Remy, A. Wagner, *Org. Biomol. Chem.* **2016**, *14*, 4794-4803.
- [53] G. Leriche, M. Nothisen, N. Baumlin, C. D. Muller, D. Bagnard, J. S. Remy, S. A. Jacques, A. Wagner, *Bioconjugate Chem.* **2015**, *26*, 1461-1465.
- [54] a) P. M. S. D. Cal, J. B. Vicente, E. Pires, A. V. Coelho, L. F. Veiros, C. Cordeiro, P. M. P. Gois, *J. Am. Chem. Soc.* **2012**, *134*, 10299-10305; b) O. Dilek, Z. Lei, K. Mukherjee, S. Bane, *Chem. Commun.* **2015**, *51*, 16992-16995.
- [55] a) P. M. S. D. Cal, R. F. M. Frade, V. Chudasama, C. Cordeiro, S. Caddick, P. M. P. Gois, *Chem. Commun.* **2014**, *50*, 5261-5263; b) J. P. M. António, R. Russo, C. Parente Carvalho, P. M. S. D. Cal, P. M. P. Gois, *Chem. Soc. Rev.* **2019**, DOI: 10.1039/C9CS00184K.
- [56] R. M. R. M. Lopes, A. E. Ventura, L. C. Silva, H. Faustino, P. M. P. Gois, *Chem. Eur. J.* **2018**, *24*, 12495-12499.
- [57] H. Gu, T. I. Chio, Z. Lei, R. J. Staples, J. S. Hirschi, S. Bane, *Org. Biomol. Chem.* **2017**, *15*, 7543-7548.
- [58] T. I. Chio, H. Gu, K. Mukherjee, L. N. Tumey, S. L. Bane, *Bioconjugate Chem.* **2019**, *30*, 1554-1564.
- [59] J. Roy, M. Kaake, M. Srinivasarao, P. S. Low, *Bioconjugate Chem.* **2018**, *29*, 2208-2214.
- [60] a) J. Z. Du, X. J. Du, C. Q. Mao, J. Wang, *J. Am. Chem. Soc.* **2011**, *133*, 17560-17563; b) P. T. Wong, S. K. Choi, *Chem. Rev.* **2015**, *115*, 3388-3432; c) Y. Kim, E. J. Park, D. H. Na, *Arch. Pharm. Res.* **2018**, *41*, 571-582.
- [61] a) M. C. Garnett, *Adv. Drug Deliv. Rev.* **2001**, *53*, 171-216; b) W. C. Shen, H. J. Ryser, *Biochem. Biophys. Res. Commun.* **1981**, *102*, 1048-1054.
- [62] S. Su, F. S. Du, Z. C. Li, *Org. Biomol. Chem.* **2017**, *15*, 8384-8392.
- [63] A. Zhang, L. Yao, M. An, *Chem. Commun.* **2017**, *53*, 12826-12829.
- [64] a) C. J. Choy, J. J. Geruntho, A. L. Davis, C. E. Berkman, *Bioconjugate Chem.* **2016**, *27*, 824-830; b) C. J. Choy, C. R. Ley, A. L. Davis, B. S. Backer, J. J. Geruntho, B. H. Clowers, C. E. Berkman, *Bioconjugate Chem.* **2016**, *27*, 2206-2213.
- [65] A. Alouane, R. Labrière, T. Le Saux, F. Schmidt, L. Jullien, *Angew. Chem.* **2015**, *127*, 7600-7619; *Angew. Chem. Int. Ed.* **2015**, *54*, 7492-7509.
- [66] A. Raposo Moreira Dias, L. Bodero, A. Martins, D. Arosio, S. Gazzola, L. Belvisi, L. Pignataro, C. Steinkühler, A. Dal Corso, C. Gennari, U. Piarulli, *ChemMedChem* **2019**, *14*, 938-942.
- [67] L. R. Staben, S. G. Koenig, S. M. Lehar, R. Vandlen, D. Zhang, J. Chuh, S. F. Yu, C. Ng, J. Guo, Y. Liu, A. Fourie-O'Donohue, M. Go, X. Linghu, N. L. Segraves, T. Wang, J. Chen, B. Wei, G. D. Phillips, K. Xu, K. R. Kozak, S. Mariathasan, J. A. Flygare, T. H. Pillow, *Nat. Chem.* **2016**, *8*, 1112-1119.
- [68] D. Zhang, H. Le, J. D. Cruz-Chuh, S. Bobba, J. Guo, L. Staben, C. Zhang, Y. Ma, K. R. Kozak, G. D. Lewis Phillips, B. S. Vollmar, J. D. Sadowsky, R. Vandlen, B. Wei, D. Su, P. Fan, P. S. Dragovich, S. C. Khojasteh, C. E. C. A. Hop, T. H. Pillow, *Bioconjugate Chem.* **2018**, *29*, 267-274.
- [69] W. Dokter, R. Ubink, M. van der Lee, M. van der Vleuten, T. van Achterberg, D. Jacobs, E. Loosveld, D. van den Dobbelaars, D. Egging, E. Mattaar, P. Groothuis, P. Beusker, R. Coumans, R. Elgersma, W. Menge, J. Joosten, H. Spijker, T. Huijbregts, V. de Groot, M. Eppink, G. de Roo, G. Verheijden, M. Timmers, *Mol. Cancer Ther.* **2014**, *13*, 2618-2629.
- [70] S. F. Yu, B. Zheng, M. Go, J. Lau, S. Spencer, H. Raab, R. Soriano, S. Jhunjunwala, R. Cohen, M. Caruso, P. Polakis, J. Flygare, A. G. Polson, *Clin. Cancer Res.* **2015**, *21*, 3298-3306.
- [71] N. Pessah, M. Reznik, M. Shamis, F. Yantiri, H. Xin, K. Bowdish, N. Shomron, G. Ast, D. Shabat, *Bioorg. Med. Chem.* **2004**, *12*, 1859-1866.
- [72] V. K. Kolakowski, K. T. Haelsig, K. K. Emmerton, C. I. Leiske, J. B. Miyamoto, J. H. Cochran, R. P. Lyon, P. D. Senter, S. C. Jeffrey, *Angew. Chem. Int. Ed.* **2016**, *55*, 7948-7951; *Angew. Chem.* **2016**, *128*, 8080-8083.



- [73] a) N. Karton-Lifshin, D. Shabat, *New J. Chem.* **2012**, *36*, 386-393; b) D. V. Santi, E. L. Schneider, G. W. Ashley, *J. Med. Chem.* **2014**, *57*, 2303-2314.
- [74] U. Y. Lau, L. T. Benoit, N. S. Stevens, K. K. Emmerton, M. Zaval, J. H. Cochran, P. D. Senter, *Mol. Pharmaceutics* **2018**, *15*, 4063-4072.
- [75] Y. Ogitani, T. Aida, K. Hagihara, J. Yamaguchi, C. Ishii, N. Harada, M. Soma, H. Okamoto, M. Oitate, S. Arakawa, T. Hirai, R. Atsumi, T. Nakada, I. Hayakawa, Y. Abe, T. Agatsuma, *Clin. Cancer Res.* **2016**, *22*, 5097-5108.
- [76] J. C. Kern, D. Dooney, R. Zhang, L. Liang, P. E. Brandish, M. Cheng, G. Feng, A. Beck, D. Bresson, J. Firdos, D. Gately, N. Knudsen, A. Manibusan, Y. Sun, R. M. Garbaccio, *Bioconjugate Chem.* **2016**, *27*, 2081-2088.
- [77] a) T. Zhao, L. Chen, Q. Li, X. Li, *Mater. Chem. B* **2018**, *6*, 7112-7121; b) D. F. Costa, L. P. Mendes, V. P. Torchilin, *Adv. Drug Deliv. Rev.* **2019**, *138*, 105-116.
- [78] B. M. Luby, C. D. Walsh, G. Zheng, *Angew. Chem. Int. Ed.* **2019**, *25*, 2558-2569; *Angew. Chem.* **2019**, *131*, 2580-2591.
- [79] J. Olejniczak, C. J. Carling, A. Almutairi, *J. Controlled Release* **2015**, *219*, 18-30.
- [80] A. Gandioso, M. Cano, A. Massaguer, V. Marchán, *J. Org. Chem.* **2016**, *81*, 11556-11564.
- [81] M. J. Hansen, F. M. Feringa, P. Kobauri, W. Szymanski, R. H. Medema, B. L. Feringa, *J. Am. Chem. Soc.* **2018**, *140*, 13136-13141.
- [82] The quantum yield is used to estimate the uncaging efficiency and it is defined as the ratio between the molar amount of released substrate and the amount of photons at the radiation wavelength absorbed by the caged compound, see: P. Klán, T. Šolomek, C. G. Bochet, A. Blanc, R. Givens, M. Rubina, V. Popik, A. Kostikov, J. Wirz, *Chem. Rev.* **2013**, *113*, 119-191. For additional examples of photoreaction quantum yields, see: a) T. Stanina, P. Shrestha, E. Palao, D. Kand, J. Peterson, A. S. Dutton, N. Rubinstein, R. Weinstein, A. H. Winter, P. Klán, *J. Am. Chem. Soc.* **2017**, *139*, 15168-15175; b) G. Bassolino, C. Nançoz, Z. Thiel, E. Bois, E. Vauthey, P. Rivera-Fuentes, *Chem. Sci.* **2018**, *9*, 387-391.
- [83] Z. Chen, B. Li, X. Xie, F. Zeng, S. Wu, *J. Mater. Chem. B* **2018**, *6*, 2547-2556.
- [84] W. Feng, C. Gao, W. Liu, H. Ren, C. Wang, K. Ge, S. Li, G. Zhou, H. Li, S. Wang, G. Jia, Z. Li, J. Zhang, *Chem. Commun.* **2016**, *52*, 9434-9437.
- [85] G. Yang, J. Liu, Y. Wu, L. Feng, Z. Liu, *Coord. Chem. Rev.* **2016**, *320*, 321, 100-117
- [86] Y. Liu, P. Bhattarai, Z. Dai, X. Chen, *Chem. Soc. Rev.* **2019**, *48*, 2053-2108.
- [87] a) A. Y. Rwei, W. Wang, D. S. Kohane, *Nano Today* **2015**, *10*, 451-467; b) P. T. Wong, S. Tang, J. Cannon, D. Chen, R. Sun, J. Lee, J. Phan, K. Tao, K. Sun, B. Chen, J. R. Baker, S. K. Choi, *Bioconjugate Chem.* **2017**, *28*, 3016-3028.
- [88] E. Cueto Díaz, S. Picard, M. Klausen, V. Hugues, P. Pagano, E. Genin, M. Blanchard-Desce, *Chem. Eur. J.* **2016**, *22*, 10848-10859.
- [89] a) Q. Lin, L. Yang, Z. Wang, Y. Hua, D. Zhang, B. Bao, C. Bao, X. Gong, L. Zhu, *Angew. Chem. Int. Ed.* **2018**, *57*, 3722-3726; *Angew. Chem.* **2018**, *130*, 3784-3788; b) A. Gandioso, S. Contreras, I. Melnyk, J. Oliva, S. Nonell, D. Velasco, J. García-Amorós, V. Marchán, *J. Org. Chem.* **2017**, *82*, 5398-5408; c) M. Klausen, V. Dubois, G. Clermont, C. Tonnelé, F. Castet, M. Blanchard-Desce, *Chem. Sci.* **2019**, *10*, 4209-4219.
- [90] J. A. Peterson, C. Wijesooriya, E. J. Gehrmann, K. M. Mahoney, P. P. Goswami, T. R. Albright, A. Syed, A. S. Dutton, E. A. Smith, A. H. Winter, *J. Am. Chem. Soc.* **2018**, *140*, 7343-7346.
- [91] A. P. Gorka, R. R. Nani, M. J. Schnermann, *Acc. Chem. Res.* **2018**, *51*, 3226-3235.
- [92] A. P. Gorka, R. R. Nani, J. Zhu, S. Mackem, M. J. Schnermann, *J. Am. Chem. Soc.* **2014**, *136*, 14153-14159.
- [93]  $t_{10\%}$  = time to 10% reaction conversion.
- [94] R. R. Nani, A. P. Gorka, T. Nagaya, T. Yamamoto, J. Ivanic, H. Kobayashi, M. J. Schnermann, *ACS Cent. Sci.* **2017**, *3*, 329-337.
- [95] T. Nagaya, A. P. Gorka, R. R. Nani, S. Okuyama, F. Ogata, Y. Maruoka, P. L. Choyke, M. J. Schnermann, H. Kobayashi, *Mol. Cancer Ther.* **2018**, *17*, 661-670.
- [96] a) T. Yamamoto, D. R. Caldwell, A. Gandioso, M. J. Schnermann, *Photochem. Photobiol.* **2019**, DOI: 10.1111/php.13090; b) J. P. Mathew, A. Greer, *Photochem. Photobiol.* **2019**, DOI: 10.1111/php.13102.
- [97] a) Z. Li, B. F. Krippendorff, S. Sharma, A. C. Walz, T. Lavé, D. K. Shah, *mAbs* **2016**, *8*, 113-119; b) A. C. Freise, A. M. Wu, *Mol. Immunol.* **2015**, *67*, 142-152.
- [98] S. Cazzamalli, A. Dal Corso, F. Widmayer, D. Neri, *J. Am. Chem. Soc.* **2018**, *140*, 1617-1621.
- [99] a) C. J. Springer, I. Niculescu-Duvaz, *Adv. Drug Deliv. Rev.* **1997**, *26*, 151-172; b) D. Shabat, C. Rader, B. List, R. A. Lerner, C. F. Barbas, *Proc. Natl. Acad. Sci. USA* **1999**, *96*, 6925-6930.
- [100] S. K. Sharma, K. D. Bagshawe, *Adv. Drug Deliv. Rev.* **2017**, *118*, 2-7.
- [101] For an excellent analysis of rate constants in bioorthogonal reactions, see: K. Lang, J. W. Chin, *ACS Chem. Biol.* **2014**, *9*, 16-20.
- [102] R. van Brakel, R. C. Vulders, R. J. Bokdam, H. Grüll, M. S. Robillard, *Bioconjugate Chem.* **2008**, *19*, 714-718.
- [103] A. S. Cohen, E. A. Dubikovskaya, J. S. Rush, C. R. Bertozzi, *J. Am. Chem. Soc.* **2010**, *132*, 8563-8565.
- [104] R. Rossin, M. S. Robillard, *Curr. Opin. Chem. Biol.* **2014**, *21*, 161-169.
- [105] a) B. L. Oliveira, Z. Guo, G. J. L. Bernardes, *Chem. Soc. Rev.* **2017**, *46*, 4895-4950; b) E. J. L. Stéen, P. E. Edem, K. Nørregaard, J. T. Jørgensen, V. Shalgunov, A. Kjaer, M. M. Herth, *Biomaterials* **2018**, *179*, 209-245.
- [106] B. L. Oliveira, Z. Guo, G. J. L. Bernardes, *Chem. Soc. Rev.* **2017**, *46*, 4895-4950.
- [107] a) X. Ji, Z. Pan, B. Yu, L. K. De La Cruz, Y. Zheng, B. Ke, B. Wang, *Chem. Soc. Rev.* **2019**, *48*, 1077-1094; b) J. Tu, M. Xu, R. M. Franzini, *ChemBioChem* **2019**, *20*, 1615-1627.
- [108] R. M. Versteegen, R. Rossin, W. ten Hoeve, H. M. Janssen, M. S. Robillard, *Angew. Chem. Int. Ed.* **2013**, *52*, 14112-14116; *Angew. Chem.* **2013**, *125*, 14362-14366.
- [109] J. C. T. Carlson, H. Mikula, R. Weissleder, *J. Am. Chem. Soc.* **2018**, *140*, 3603-3612.
- [110] R. M. Versteegen, W. Ten Hoeve, R. Rossin, M. A. R. de Geus, H. M. Janssen, M. S. Robillard, *Angew. Chem. Int. Ed.* **2018**, *57*, 10494-10499; *Angew. Chem.* **2018**, *130*, 10654-10659.
- [111] A. J. C. Sarris, T. Hansen, M. A. R. de Geus, E. Maurits, W. Doelman, H. S. Overkleeft, J. D. C. Codée, D. V. Filippov, S. I. van Kasteren, *Chem. Eur. J.* **2018**, *24*, 18075-18081.
- [112] R. Rossin, S. M. van den Bosch, W. ten Hoeve, M. Carvelli, R. M. Versteegen, J. Lub, M. S. Robillard, *Bioconjugate Chem.* **2013**, *24*, 1210-1217.
- [113] M. R. Karver, R. Weissleder, S. A. Hilderbrand, *Bioconjugate Chem.* **2011**, *22*, 2263-2270.
- [114] R. Rossin, R. M. Versteegen, J. Wu, A. Khasanov, H. J. Wessels, E. J. Steenbergen, W. Ten Hoeve, H. M. Janssen, A. H. A. M. van Onzen, P. J. Hudson, M. S. Robillard, *Nat. Commun.* **2018**, *9*, 1484.
- [115] Q. Yao, F. Lin, X. Fan, Y. Wang, Y. Liu, Z. Liu, X. Jiang, P. R. Chen, Y. Gao, *Nat. Commun.* **2018**, *9*, 5032.
- [116] S. S. Matikonda, D. L. Orsi, V. Staudacher, I. A. Jenkins, F. Fiedler, J. Chen, A. B. Gamble, *Chem. Sci.* **2015**, *6*, 1212-1218.
- [117] M. Xu, J. Tu, R. M. Franzini, *Chem. Commun.* **2017**, *53*, 6271-6274.
- [118] J. Tu, M. Xu, S. Parvez, R. T. Peterson, R. M. Franzini, *J. Am. Chem. Soc.* **2018**, *140*, 8410-8414.
- [119] a) H. Wu, S. C. Alexander, S. Jin, N. K. Devaraj, *J. Am. Chem. Soc.* **2016**, *138*, 11429-11432; b) K. Neumann, S. Jain, A. Gambardella, S. E. Walker, E. Valero, A. Lilienkamp, M. Bradley, *ChemBioChem* **2017**, *18*, 91-95; c) E. Jiménez-Moreno, Z. Guo, B. L. Oliveira, I. S. Albuquerque, A. Kitowski, A. Guerreiro, O. Boutoureira, T. Rodrigues, G. Jiménez-Osés, G. J. L. Bernardes, *Angew. Chem. Int. Ed.* **2017**, *56*, 243-247; *Angew. Chem.* **2017**, *129*, 249-253.
- [120] S. Cazzamalli, B. Ziffels, F. Widmayer, P. Murer, G. Pellegrini, F. Pretto, S. Wulfhart, D. Neri, *Clin. Cancer Res.* **2018**, *24*, 3656-3667.